Distribution Category:
Water Reactor Safety
Research--Analysis
Development (NRC-4)

ANL-77-47

ARGONNE NATIONAL LABORATORY
9700 South Cass Avenue
Argonne, Illinois 60439

ONE-DIMENSIONAL DRIFT-FLUX MODEL AND CONSTITUTIVE EQUATIONS FOR RELATIVE MOTION BETWEEN PHASES IN VARIOUS TWO-PHASE FLOW REGIMES

by

M. Ishii

Reactor Analysis and Safety Division

October 1977

DISCLAIMER

TABLE OF CONTENTS

LIST OF FIGURES

LIST OF FIGURES

LIST OF TABLES

NOMENCLATURE

A	Total flow area
A_d	Projected area of a particle
a	Parameter defined by Eq. 89
b	Parameter defined by Eq. 89
C_D	Drag coefficient for multiparticle system
$C_{D\infty}$	Drag coefficient for single-particle system
C_0	Distribution parameter
C_∞	Asymptotic value of C_0
C_{hk}	Enthalpy-distribution parameter for k phase
C_{hm}	Enthalpy-distribution parameter for mixture
C_{vk}	Momentum-distribution parameter for k phase
C_{vm}	Momentum-distribution parameter for mixture
c	Parameter defined by Eq. 89
C_D'	Drag coefficient in churn-flow regime based on V_{dj}
$C_{\psi k}$	Distribution parameter for property ψ_k
D	Hydraulic diameter
E_d	Area fraction of liquid entrained in the gas core based on liquid area
$f(\alpha_d)$	Given function of void fraction
f_m	Mixture friction factor
f_i	Interfacial friction factor
f_{wf}	Wall friction factor for liquid film
F_p	Pressure force
F_g	Gravity force
F_D	Drag force
G	Total mass flow rate
g	Gravity
g_z	Axial component of gravity
g^*	Nondimensional gravity parameter
h_k	Enthalpy of k phase
h_m	Enthalpy of mixture
h_{msat}	Enthalpy of saturation mixture
h_0	Enthalpy at centerline
h_w	Enthalpy at wall
h_{ks}	Saturation enthalpy of k phase
j_{core}	Total volumetric flux based on the core area
$\langle j_f \rangle_{tr}$	Liquid flux at the laminar turbulent transition
j_g^*	Nondimensional gas flux; $j_g/\sqrt{\Delta\rho g D/\rho_g}$
j_0	Volumetric flux at centerline
j	Mixture volumetric flux
j_k	Volumetric flux of k phase
K	Kutateladze number
m	Exponent of power profile of properties
M_{ik}	Interfacial drag force of k phase
$M_{\tau k}$	Transverse stress gradient of k phase
$M_{\tau m}$	Mixture transverse stress gradient
M_τ^*	Nondimensional stress-gradient parameter
N_μ	Viscosity number based on continuous-phase viscosity
$N_{\mu f}$	Viscosity number based on liquid viscosity
$N_{Re\infty}$	Single-particle Reynolds number
N_{Re}	Particle Reynolds number
n	Exponent of power profile of properties
p	Pressure
P_i	Wetted perimeter of interface
P_{wf}	Wetted perimeter of wall for liquid phase
q_w''	Wall heat flux
$\vec{q}$	Conduction heat flux
$\vec{q}_T$	Turbulent heat flux
q_{cr}''	Critical heat flux
Q_k	Volumetric flow of k phase
R	Radial coordinate
r_d	Particle radius
r_d^*	Nondimensional radius
R_w	Radius of pipe
Re_f	Film Reynolds number

NOMENCLATURE

t	Time
v_{fc}	Liquid drop velocity in annular core
v_{ff}	Liquid film velocity
v_{gc}	Gas-core velocity
$\vec{V}_{dj}$	Local drift velocity
$\langle\langle V_{dj} \rangle\rangle$	Weighted mean of local drift velocity
$\bar{V}_{dj}$	Mean transport drift velocity
v_m	Mixture velocity
v_k	Velocity of k phase
v_r	Relative velocity
$v_{r\infty}$	Terminal velocity for single-particle system
v^*	Nondimensional velocity
V_d	Volume of particle
y	Distance from the wall
z	Axial coordinate
α	Gas (vapor) void fraction
α_k	Void fraction of k phase
α_{dm}	Maximum packing void fraction
α_{dw}	Void fraction of dispersed phase at wall
α_{d0}	Void fraction of dispersed phase at centerline
α_{core}	Fraction of area occupied by annular core
α_{drop}	Fraction of area occupied by droplets from annular core area
α_{kw}	Void fraction of k phase at wall
α_{k0}	Void fraction of k phase at centerline
Γ_k	Mass Source for k phase
δ	Thickness of liquid film
$\Delta\alpha_k$	Difference of void fraction at center and wall
$\Delta\psi_{dc}$	Property difference between d and c phases
Δh_{dc}	Enthalpy difference, $h_d - h_c$
$\Delta\rho$	Absolute value of density difference
μ_k	Viscosity of k phase
μ_m	Mixture viscosity in dispersed flow
ξ_h	Heated perimeter
ξ	Ratio of wetted perimeters, P_i/P_{wf}
ρ_k	Density of k phase
ρ_m	Density of mixture
σ	Surface tension
$\bar{\bar{\tau}}$	Averaged viscous stress for mixture
$\bar{\bar{\tau}}^T$	Turbulent stress for mixture
$\bar{\bar{\tau}}_k$	Averaged viscous stress for k phase
$\bar{\bar{\tau}}_k^T$	Turbulent stress for k phase
$\bar{\bar{\tau}}_{ki}$	Average interfacial stress for k phase
τ_i	Axial shear force at annular interface
τ_{wf}	Wall shear force for liquid film
τ_{zz}	Normal viscous stress
τ_{zz}^T	Normal turbulent stress
Φ_m^μ	Mixture-energy dissipation
ψ	Given function of r_d^*
ψ_k	Property of k phase
ψ_m	Mixture Property

Subscripts

c	Continuous phase
d	Dispersed phase
f	Liquid phase
g	Vapor or gas phase
k	k phase (k = c,d or k = g,f)
ki	k phase at interface
m	Mixture

Symbols

$\langle\psi\rangle$	Area average
$\langle\langle\psi_k\rangle\rangle$	Weighted mean value
ψ_m	Weighted mean mixture property
COV	Covariance
*	Nondimensional

ONE-DIMENSIONAL DRIFT-FLUX MODEL AND CONSTITUTIVE EQUATIONS FOR RELATIVE MOTION BETWEEN PHASES IN VARIOUS TWO-PHASE FLOW REGIMES

by

M. Ishii

ABSTRACT

In view of the practical importance of the drift-flux model for two-phase flow analysis in general and in the analysis of nuclear-reactor transients and accidents in particular, the kinematic constitutive equation for the drift velocity has been studied for various two-phase flow regimes. The constitutive equation that specifies the relative motion between phases in the drift-flux model has been derived by taking into account the interfacial geometry, the body-force field, shear stresses, and the interfacial momentum transfer, since these macroscopic effects govern the relative velocity between phases. A comparison of the model with various experimental data over various flow regimes and a wide range of flow parameters shows a satisfactory agreement.

I. INTRODUCTION

Two-phase flows always involves some relative motion of one phase with respect to the other; therefore, a two-phase-flow problem should be formulated in terms of two velocity fields. A general transient two-phase-flow problem can be formulated by using a two-fluid model or a drift-flux model, depending on the degree of the dynamic coupling between the phases. In the two-fluid model, each phase is considered separately; hence the model is formulated in terms of two sets of conservation equations governing the balance of mass, momentum, and energy of each phase. However, an introduction of two momentum equations in a formulation, as in the case of the two-fluid model, presents considerable difficulties because of mathematical complications and of uncertainties in specifying interfacial interaction terms between two phases.[1-4] Numerical instabilities caused by improper choice of interfacial-interaction terms in the phase-momentum equations are common; therefore careful studies on the interfacial constitutive equations are required in the formulation of the two-fluid model. For example, it has been suggested[5] that the interaction terms should include first-order time and spatial derivatives under certain conditions.

These difficulties associated with a two-fluid model can be significantly reduced by formulating two-phase problems in terms of the drift-flux model,[6] in which the motion of the whole mixture is expressed by the mixture-momentum equation and the relative motion between phases is taken into account by a kinematic constitutive equation. Therefore, the basic concept of the drift-flux model is to consider the mixture as a whole, rather than as two separated phases. The formulation of the drift-flux model based on the mixture balance equations is simpler than the two-fluid model based on the separate balance equations for each phase. The most important assumption associated with the drift-flux model is that the dynamics of two phases can be expressed by the mixture-momentum equation with the kinematic constitutive equation specifying the relative motion between phases. The use of the drift-flux model is appropriate when the motions of two phases are strongly coupled.

In the drift-flux model, the velocity fields are expressed in terms of the mixture center-of-mass velocity and the drift velocity of the vapor phase, which is the vapor velocity with respect to the volume center of the mixture. The effects of thermal nonequilibrium are accommodated in the drift-flux model by a constitutive equation for phase change that specifies the rate of mass transfer per unit volume. Since the rates of mass and momentum transfer at the interfaces depend on the structure of two-phase flows, these constitutive equations for the drift velocity and the vapor generation are functions of flow regimes.[7,8]

The drift-flux model is an approximate formulation in comparison with the more rigorous two-fluid formulation. However, because of its simplicity and applicability to a wide range of two-phase-flow problems of practical interest, the drift-flux model is of considerable importance. In particular, the model is useful for transient thermohydraulic and accident analyses of both LWR's and LMFBR's. In view of the practical importance of the drift-flux model for two-phase-flow analyses, the kinematic constitutive equation for the drift velocity has been studied in the present analysis. The constitutive equation for the vapor-drift velocity for bubbly and slug flows has been studied by Zuber et al.[9-11] by balancing the gravity force with the drag force. The drift velocity in two-phase annular flows has been analyzed.[12] The present study is an extension of the above analysis.

II. THREE-DIMENSIONAL FORMULATION

The three-dimensional form of the drift-flux model[4] has been obtained by using the time or statistical averaging method. The result can be summarized as follows:

Mixture Continuity Equation:

$$\frac{\partial \rho_m}{\partial t} + \nabla\cdot(\rho_m \vec{v}_m) = 0. \qquad (1)$$

Continuity Equation for Dispersed Phase:

$$\frac{\partial \alpha_d \rho_d}{\partial t} + \nabla\cdot(\alpha_d \rho_d \vec{v}_m) = \Gamma_d - \nabla\cdot\left(\frac{\alpha_d \rho_d \rho_c}{\rho_m}\vec{V}_{dj}\right). \tag{2}$$

Mixture Momentum Equation:

$$\frac{\partial \rho_m \vec{v}_m}{\partial t} + \nabla\cdot(\rho_m \vec{v}_m \vec{v}_m) = -\nabla p_m + \nabla\cdot\left(\bar{\bar{\tau}} + \bar{\bar{\tau}}^T - \frac{\alpha_d}{1-\alpha_d}\frac{\rho_d \rho_c}{\rho_m}\vec{V}_{dj}\vec{V}_{dj}\right) + \rho_m \vec{g}. \tag{3}$$

Mixture Enthalpy-energy Equation:

$$\frac{\partial \rho_m h_m}{\partial t} + \nabla\cdot(\rho_m h_m \vec{v}_m) = -\nabla\cdot\left[\vec{q} + \vec{q}^T + \frac{\alpha_d \rho_d \rho_c}{\rho_m}(h_d - h_c)\vec{V}_{dj}\right] + \frac{\partial p_m}{\partial t} + \left[\vec{v}_m + \frac{\alpha_d(\rho_c - \rho_d)}{\rho_m}\vec{V}_{dj}\right]\cdot\nabla p_m + \Phi_m^{\mu}. \tag{4}$$

Here α_k, ρ_k, h_k, $\bar{\bar{\tau}}$, and $\vec{q}$ are the conventional time- (or ensemble)-averaged local void fraction, phase density, phase enthalpy, viscous stress, and conduction heat flux, respectively. The component k denotes either the continuous (k = c) or the dispersed phase (k = d); ρ_m, $\vec{v}_m$, p_m, and h_m are the local mean density, velocity, pressure, and enthalpy of the mixture, respectively; $\bar{\bar{\tau}}^T$ and $\vec{q}^T$ are the turbulent diffusion flux of momentum and energy for the mixture; Γ_k is the mass-transfer term for phase k due to phase changes; and Φ_m^{μ} is the energy-dissipation term. The velocity $\vec{V}_{dj}$ denotes the drift velocity of the dispersed phase; its physical significance is explained below.

The center-of-mass velocity of the mixture is given by

$$\vec{v}_m \equiv [\alpha_d \rho_d \vec{v}_d + (1-\alpha_d)\rho_c \vec{v}_c]/\rho_m, \tag{5}$$

where $\vec{v}_d$ and $\vec{v}_c$ are the mass-weighted mean velocities of phases d and c. The velocity of the center of volume of the mixture is

$$j \equiv \alpha_d \vec{v}_d + (1-\alpha_d)\vec{v}_c = \vec{j}_d + \vec{j}_c, \tag{6}$$

where $\vec{j}_d$ and $\vec{j}_c$ are the local volumetric fluxes of the indicated phases. The vapor drift velocity of a dispersed phase is the velocity of the dispersed phase with respect to the volume center of the mixture:

$$\vec{V}_{dj} = \vec{v}_d - \vec{j} = (1-\alpha_d)(\vec{v}_d - \vec{v}_c) = (1-\alpha_d)\vec{v}_r, \tag{7}$$

where $\vec{v}_r$ is the relative velocity between phases. In Eqs. 2-4, the convective terms are formulated in terms of $\vec{v}_m$; therefore, an additional diffusion flux due to relative motion between phases appears on the right-hand side of the equations. To take these diffusion effects into account, the drift velocity should be specified by kinematic constitutive equations, which may be written as

$$\vec{V}_{dj} = \vec{V}_{dj}(\alpha_d, p_m, \vec{g}, \vec{v}_m, \text{etc.}). \tag{8}$$

To take into account the mass transfer across the interfaces, a constitutive equation for Γ_d should also be given. In a functional form, this phase-change constitutive equation may be written as

$$\Gamma_d = \Gamma_d(\alpha_d, p_m, \vec{v}_m, \frac{\partial p_m}{\partial t}, h_m - h_{msat}, \text{etc.}). \tag{9}$$

The vapor-drift velocity in the drift-flux model plays a role similar to that of the diffusion coefficient in a single-phase two-component system. However, the application of a diffusion coefficient is useful only when the relative motion between components or phases is due to a concentration gradient and can be expressed by a linear constitutive law. For general two-phase flow systems, Fick's law of diffusion may not hold, since in this case the interfacial geometry, the body-force field, and the interfacial momentum transfer are the factors governing the relative motion of phases. In other words, in two-phase systems, the diffusion of phases is macroscopic, whereas in single-phase two-component systems, it is due to the microscopic molecular diffusion. The constitutive equation for the vapor-drift velocity is therefore expected to depend strongly on the two-phase flow regimes, since the momentum transfer between the phases is governed by the geometry of the interfaces as well as by the interfacial-area concentration.

III. MULTIPARTICLE SYSTEM IN INFINITE MEDIA

The relative motion between phases can be studied by considering the momentum equations for each phase in the two-fluid-model formulation. In a three-dimensional form, the k-phase momentum equation[4] is given by

$$\alpha_k\rho_k\left(\frac{\partial\vec{v}_k}{\partial t} + \vec{v}_k\cdot\nabla\vec{v}_k\right) = -\alpha_k\nabla p_k + \alpha_k\nabla\cdot\left(\bar{\bar{\tau}}_k + \bar{\bar{\tau}}_k^T\right) + \alpha_k\rho_k\vec{g} + (p_{ki} - p_k)\nabla\alpha_k$$
$$- (\nabla\alpha_k)\cdot\left[\bar{\bar{\tau}}_{ki} - \left(\bar{\bar{\tau}}_k + \bar{\bar{\tau}}_k^T\right)\right] + (\vec{v}_{ki} - \vec{v}_k)\Gamma_k + \vec{M}_{ik}, \tag{10}$$

where the subscript ki denotes the value at the interface for phase k and $\vec{M}_{ik}$ is the interfacial drag force. Under the assumption that the averaged pressure and stress in the bulk fluid and at the interface are approximately the same, we obtain

$$\alpha_k \rho_k \left(\frac{\partial \vec{v}_k}{\partial t} + \vec{v}_k \cdot \nabla \vec{v}_k \right) = -\alpha_k \nabla p_k + \alpha_k \nabla \cdot \left(\bar{\bar{\tau}}_k + \bar{\bar{\tau}}_k^T \right) + \alpha_k \rho_k \vec{g} + \vec{M}_{ik} + (\vec{v}_{ki} - \vec{v}_k) \Gamma_k. \tag{11}$$

The conservation of the mixture momentum requires

$$\sum_k \vec{M}_{ik} = 0, \tag{12}$$

which is the modified form of the averaged momentum-jump condition.

The two-fluid formulation for dispersed two-phase flow system was used by Carrier[13] and Rannie,[14] among others, in relation to low-concentration flows through rocket nozzles. The problems were analyzed by considering the equations of motion for a particle and mixture with a relatively simple interaction term between phases. However, for flows with high concentrations and under rapid transient conditions, some modification of the analysis is required to apply the two-fluid model.

Now let us consider the derivation of the drift velocity from the two-fluid model. In the absence of the wall and under a steady-state condition without phase change ($\Gamma_k = 0$), the multiparticle system in an infinite medium essentially reduces to a gravity-dominated one-dimensional flow, since the average void and velocity profiles become flat. Then the axial component of the momentum equation for k phase can be written as

$$0 = -\alpha_k \frac{dp_m}{dz} - \alpha_k \rho_k g + M_{ik}. \tag{13}$$

Here we have also assumed that the surface-tension effect can be neglected, and therefore $p_c = p_d = p_m$. By adding the phase-momentum equations and using Eq. 12, we obtain

$$\frac{dp_m}{dz} = -\rho_m g. \tag{14}$$

The drag force acting on the particle under steady-state condition can be given in terms of the drag coefficient C_D based on the relative velocity as

$$F_D = -\tfrac{1}{2} C_D \rho_c v_r |v_r| A_d, \tag{15}$$

where A_d is the projected area of a typical particle. Then F_D is related to the interfacial force by

$$F_D = M_{id} V_d / \alpha_d, \tag{16}$$

where V_d is the volume of a particle. Then from Eqs. 13-15, we obtain

$$v_r |v_r| = \frac{8}{3} \frac{r_d}{C_D \rho_c} (\rho_c - \rho_d) g (1 - \alpha_d), \tag{17}$$

where the mean radius of the particle is defined by $r_d = 3V_d/(4A_d)$.

On the other hand, for a single-particle system in an infinite medium, the force balance (as shown in the appendix) reduces to

$$v_{r\infty} |v_{r\infty}| = \frac{8}{3} \frac{r_d}{C_{D\infty} \rho_c} (\rho_c - \rho_d) g, \tag{18}$$

Where $v_{r\infty}$ and $C_{D\infty}$ are the terminal velocity and drag coefficient of a single particle in an infinite medium. In general, the drag law for a single particle can be expressed by $C_{D\infty} = C_{D\infty}(N_{Re\infty})$, where the Reynolds number $N_{Re\infty}$ is given by $N_{Re\infty} \equiv 2 r_d \rho_c |v_{r\infty}| / \mu_c$. The expressions for $C_{D\infty}$ in various flow regimes are given in the appendix and shown in Fig. 1. Also, the nondimensional terminal velocity is shown as a function of the dimensionless radius of a particle in Fig. 2.

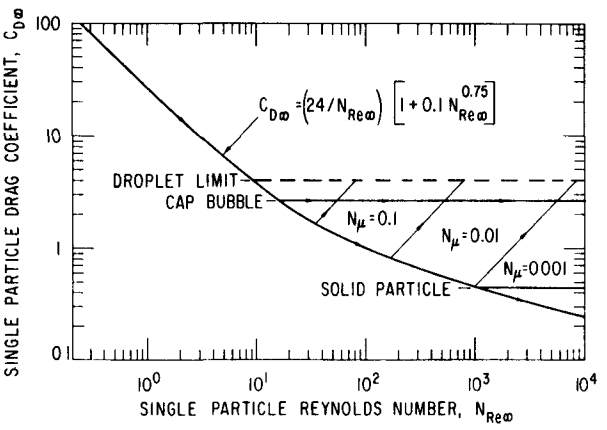

Fig. 1. Single-particle Drag Coefficient. ANL Neg. No. 900-76-443. Corr.

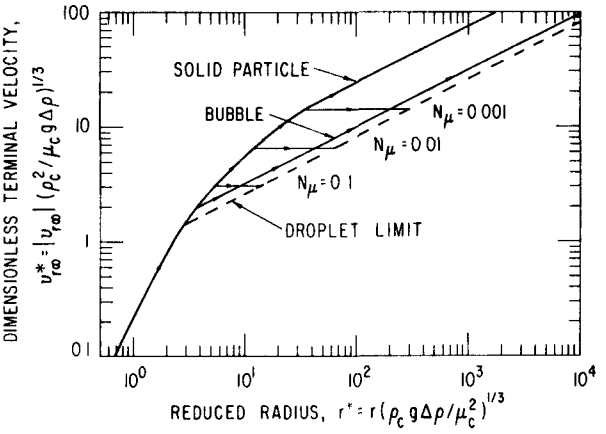

Fig. 2. Terminal Velocity. ANL Neg. No. 900-76-445.

Then from Eqs. 17 and 18, we get

$$C_{D\infty}(N_{Re\infty}) \equiv C_D(N_{Re}) \left(\frac{v_r}{v_{r\infty}}\right)^2 \Big/ (1 - \alpha_d), \tag{19}$$

where the Reynolds number is given by $N_{Re} = 2 r_d \rho_c |v_r| / \mu_m$ and μ_m is the mixture viscosity. If we know the mixture viscosity and the dependence of C_D on N_{Re}, Eq. 19 can be solved for the slip velocity in terms of the single-particle terminal velocity.

The presence of the mixture viscosity in the similarity group N_{Re} is explained as follows:[9,15] A single particle moving through a dispersed two-phase mixture imparts a motion to the continuous phase. However, as the fluid moves, its deformation causes translational and rotational motions of other particles in the neighborhood. Since the particles are more resistant to deformation than is the fluid, the particles impose a system of forces that react upon the fluid. As a result of additional stresses, the original particle sees an increase in the resistance to its motion, which appears to it as arising from an increase of the viscosity. Consequently, in an analysis of the motion of the suspended particles, the mixture viscosity should be used.[15]

In the present analysis, we have extended Taylor's correlation for the mixture viscosity along the Roscoe-type power relation based on the maximum packing α_{dm}. Thus,

$$\frac{\mu_m}{\mu_c} = \left(1 - \frac{\alpha_d}{\alpha_{dm}}\right)^{-2.5\alpha_{dm}(\mu_d+0.4\mu_c)/(\mu_d+\mu_c)} . \tag{20}$$

The maximum packing α_{dm} for solid- or liquid-particle systems ranges from 0.5 to 0.74. However, $\alpha_{dm} = 0.62$ suffices for most practical cases. For a bubbly flow, the theoretical value of α_{dm} can be much higher. Therefore, by considering the standard range of interest of the void fraction $\alpha_d < 0.35$ for developed flow and α_d higher than 0.35 in developing flows, and in view of the possible foam regime, we may take $\alpha_{dm} \simeq 1$. A similar argument can be used for a droplet flow.

Figure 3 compares the proposal for present mixture viscosity with the various existing models for solid-particle systems. Including the effect of the viscosity of the dispersed phase in the correlation gives the newly developed model an advantage over the conventional correlations, because it is not limited to particulate flows, but can also be applied to droplet and bubbly flows.

Now let us assume that in the viscous regime a complete similarity exists between $C_{D\infty}$ based on $N_{Re\infty}$ and C_D based on N_{Re}, so that C_D has exactly the same functional form in terms of N_{Re} as $C_{D\infty}$ in terms of $N_{Re\infty}$ given by Eq. A.4. Then, by considering the two asymptotic cases of $N_{Re} \to 0$ and $N_{Re} \to \infty$ and interpolating between them, we obtain, from Eq. 19,

$$\frac{v_r}{v_{r\infty}} \simeq (1 - \alpha_d)^{1/2} f(\alpha_d) \frac{1 + 0.1N_{Re\infty}^{0.75}}{1 + 0.1N_{Re\infty}^{0.75}[f(\alpha_d)]^{6/7}} , \tag{21}$$

where

$$f(\alpha_d) = (1 - \alpha_d)^{1/2}\mu_c/\mu_m . \tag{22}$$

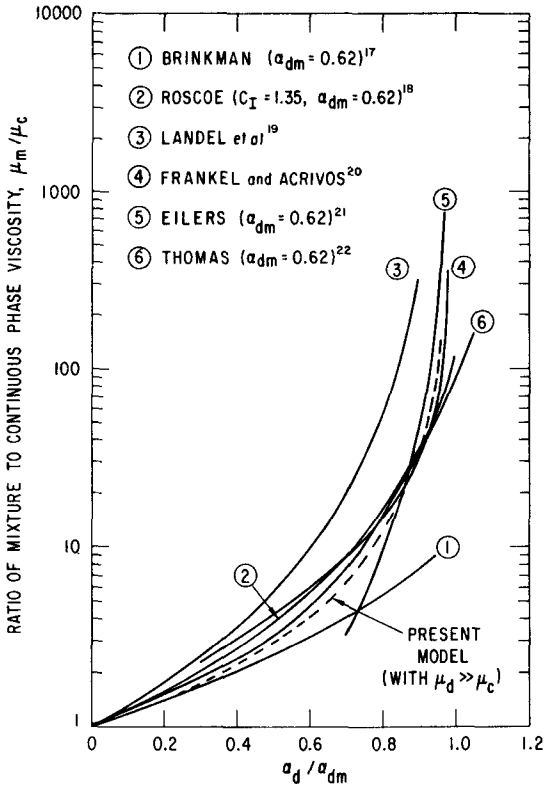

Fig. 3

Mixture-viscosity Model. ANL Neg. No. 900-76-441 Rev. 1.

Consequently, the drift velocity, which is related to the relative velocity by $V_{dj} = (1 - \alpha_d)v_r$, can be given by

$$V_{dj} \simeq v_{r\infty}(1 - \alpha_d)^{1.5} f(\alpha_d) \frac{1 + \psi(r_d^*)}{1 + \psi(r_d^*)[f(\alpha_d)]^{6/7}}, \tag{23}$$

where $\psi(r_d^*) = 0.55[(1 + 0.08 r_d^{*3})^{4/7} - 1]^{0.75}$ for the viscous regime, and r_d^* is the non-dimensional radius given by $r_d^* = r_d[\rho_c g \Delta\rho/\mu_c^2]^{1/3}$. Note that $N_{Re\infty}$ in Eq. 21 has been replaced by a new function ψ using the identity $N_{Re\infty} = 2 r_d^* v_{r\infty}^*$ and Eq. A.7.

The similarity criterion given by $C_D(N_{Re}) = C_{D\infty}(N_{Re})$ with the Reynolds number based on the mixture viscosity is first introduced for the solid-particle system in the Stokes regime.[9,16] In this case, the velocity ratio B reduces to $B = (1 - \alpha_d)\mu_c/\mu_m$, which is the limiting case of Eq. 21 with $N_{Re\infty} \ll 1$ or $r_d^* \ll 1$. However, because of the use of the generalized drag law and the mixture-viscosity model in the analysis, the present theory is not limited to a solid-particle system or to the Stokes regime.

For solid-particle systems, we assume that the transition from the viscous regime to Newton's regime occurs at the same radius as in the single-particle system, and that the drag coefficient C_D is a continuous function. Then, for Newton's regime given by $r_d^* \geq 34.65$, we obtain

$$V_{dj} = v_{r\infty}(1 - \alpha_d)^{1.5} f(\alpha_d) \frac{18.67}{1 + 17.67[f(\alpha_d)]^{6/7}}, \tag{24}$$

where $f(\alpha_d)$ is given by Eq. 22.

Figure 4 compares the above theoretical results given by Eqs. 23 and 24 with the empirical correlation for solid-particulate systems.[23] An agreement at relatively low volumetric concentrations is excellent at all Reynolds-number regions. At very high values of α_d, the present theory predicts much lower drift velocities than the Richardson-Zaki correlation.[23] However, the original experimental data of Richardson and Zaki also indicate this trend, which is predicted by the present theory, as shown in Fig. 5.

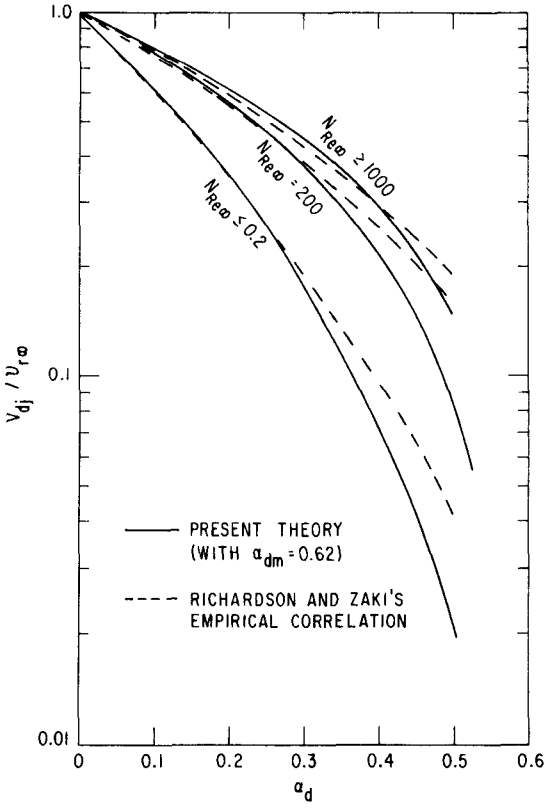

Fig. 4. Comparison of Predicted Results with Richardson and Zaki's[23] Empirical Correlations for Solid-particulate Flow Systems. ANL Neg. No. 900-76-442.

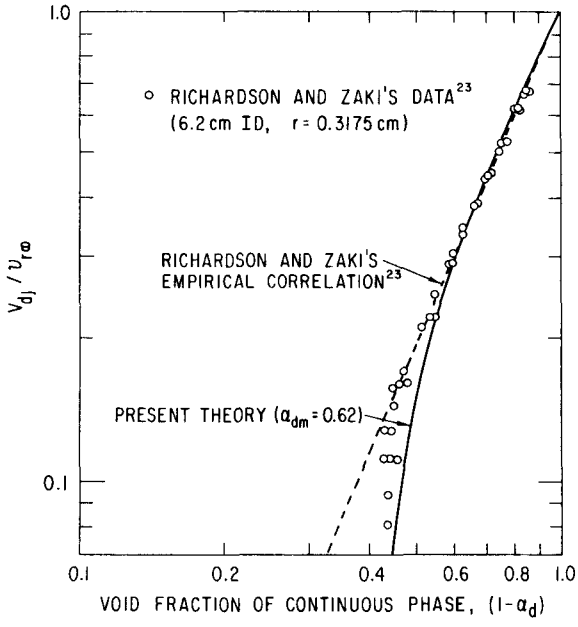

Fig. 5. Comparison of Present Model with Experimental Data for Solid Particles. ANL Neg. No. 900-76-444 Rev. 1.

In the distorted-fluid-particle regime, the single-particle drag coefficient depends only on the particle radius and fluid properties and not on the velocity or the viscosity; i.e., $C_{D\infty} = (4/3)r_d\sqrt{g\Delta\rho/\sigma}$. Thus, for a particle of a fixed diameter, $C_{D\infty}$ becomes constant. In considering the drag coefficient for a multiparticle system with the same radius, we must take into account the restrictions imposed by the existence of other particles on the flow field.

Because of the random characteristic of the turbulent eddies and particle oscillations, a particle sees the increased drag due to other particles in essentially the same way as in Newton's regime for a solid-particle system where $C_{D\infty}$ is constant under a turbulent flow condition.

Hence we postulate that, regardless of the differences in $C_{D\infty}$ in these regimes, the effect of increased drag can be predicted by the same expression. Under this assumption, Eq. 24 may also be used for the distorted-particle regime with the appropriate $v_{r\infty}$. Substituting the definition of $f(\alpha_d)$ into Eq. 24, the results can be further simplified to

$$V_{dj} \simeq v_{r\infty} \times \begin{cases} (1 - \alpha_d)^{1.75}; & \mu_c \gg \mu_d \\ (1 - \alpha_d)^2; & \mu_c \simeq \mu_d \\ (1 - \alpha_d)^{2.25}; & \mu_d \gg \mu_c \end{cases} \tag{25}$$

for the distorted-fluid-particle regime $|v_{r\infty}| = \sqrt{2}(g\sigma\Delta\rho/\rho_c^2)^{0.25}$. The above criterion is applicable for $N_\mu \geq 0.11\ (1 + \psi)/\psi^{8/3}$. For a distorted-bubbly flow the first expression under the condition $\mu_c \gg \mu_d$ is applicable, which is very close to the semiempirical correlation of Zuber and Findley;[10] i.e., $V_{dj} = v_{r\infty}(1 - \alpha_d)^{1.5}$. For $\alpha_d \ll \alpha_{dm}$, the above expression with $\mu_d \gg \mu_c$ can be used for Newton's regime with $|v_{r\infty}| = 2.43\sqrt{gr_d\Delta\rho/\rho_c}$.

As the radius of the fluid particle is further increased, the wake and bubble boundary layer can overlap due to the formation of large wake regions. In other words, a particle can influence both the surrounding fluid and other particles directly. Hence the entrainment of a particle in a wake of other particles becomes possible. This flow regime is known as the churn-turbulent-flow regime and is commonly observed in bubbly flows. In this flow regime, a typical particle moves with respect to the average volumetric flux j rather than at the average velocity of a continuous phase. Hence, the reference velocity in the definitions of the drag coefficient and the Reynolds number should be the drift velocity rather than the relative velocity.

In a churn-turbulent-flow regime, some particles should have reached the distortion limit corresponding to the cap-bubble transition or the droplet disintegration. This limit can be given by the Weber-number criterion based on the drift velocity as $2\rho_c V_{dj}^2 r_d/\sigma = 8$ (bubble) or 12 (droplet). Due to the entrainment of particles in a wake of other particles and the coalescence and disintegration caused by the turbulence, the average motion of the dispersed phase is mainly governed by those particles that satisfy the Weber-number criterion. Thus for a churn-turbulent flow, we have $F_D = -C_D'\rho_c V_{dj}|V_{dj}|\pi r_d^2/2$ with $C_D' = 8/3$. Therefore, in a standard form,

$$F_D = -\frac{C_D}{2}\rho_c v_r|v_r|\pi r_d^2, \tag{26}$$

where $C_D = 8(1 - \alpha_d)^2/3$. Hence, by balancing the drag force with the pressure and gravity forces, we obtain

$$V_{dj} = \left\{ \begin{matrix} \sqrt{2} \\ \text{or } 1.57 \end{matrix} \right\} \left(\frac{\sigma g \Delta\rho}{\rho_c^2} \right)^{1/4} \frac{\rho_c - \rho_d}{\Delta\rho} (1 - \alpha_d)^{1/4}$$

$$\simeq \sqrt{2} \left(\frac{\sigma g \Delta\rho}{\rho_c^2} \right)^{1/4} \frac{\rho_c - \rho_d}{\Delta\rho} . \qquad (27)$$

In the exact expression for V_{dj}, the proportionality constant $\sqrt{2}$ is applicable for bubbly flows and 1.57 for droplet flows. However, in view of the uncertainty in predicting the drag coefficient, this difference as well as the effect of the void fraction may be neglected. The above result is consistent with the study by Zuber and Findley for bubbly flows.[10] The present results for the drift velocity are summarized in Table I by considering four different cases: bubbles in liquid, droplets in liquid, droplets in gas, and solid particles in gas or liquid.

TABLE I. Summary of Drift Velocity V_{dj} in Infinite Media

	Bubble in Liquid	Droplet in Liquid	Droplet in Gas	Solid Particle
μ_c/μ_m	$(1 - \alpha_d)$	$\sim(1 - \alpha_d)^2$	$\sim(1 - \alpha_d)^{2.6}$	$\sim(1 - \alpha_d)^{2.6}$
Stokes Regime	$\frac{2}{9} \frac{g\Delta\rho r_d^2}{\mu_f} (1 - \alpha_d)^3$	$\frac{2}{9} \frac{g(\rho_c - \rho_d)}{\mu_c} r_d^2 (1 - \alpha_d)^2 \frac{\mu_c}{\mu_m}$		
Undistorted-particle Regime	$\frac{10.8\mu_c}{\rho_c r_d} \frac{\mu_c}{\mu_m} (1 - \alpha_d)^2 \frac{\psi^{4/3}(1 + \psi)}{1 + \psi \left[\frac{\mu_c}{\mu_m} (1 - \alpha_d)^{0.5} \right]^{6/7}} \frac{\rho_c - \rho_d}{\Delta\rho}$,			For Newton's Regime ($r_d^* \geq 34.67$),
$N_\mu \leq 0.11 \frac{1 + \psi}{\psi^{8/3}}$	where $\psi = 0.55[(1 + 0.08 r_d^{*3})^{4/7} - 1]^{0.75}$			$\psi = 17.67$
Distorted-particle Regime	$\sqrt{2} \left(\frac{\sigma g \Delta\rho}{\rho_c^2} \right) (1 - \alpha_d)^n \frac{\rho_c - \rho_d}{\Delta\rho}$			-
	$n = 1.75$	$n \simeq 2.0$	$n = 2.25$	
Churn-turbulent Regime	$\sqrt{2} \left(\frac{\sigma g \Delta\rho}{\rho_f^2} \right)^{1/4}$	$\sqrt{2} \left(\frac{\sigma g \Delta\rho}{\rho_c^2} \right)^{1/4} \frac{\rho_c - \rho_d}{\Delta\rho}$		-

IV. LOCAL DRIFT VELOCITY OF DISPERSED FLOW IN CONFINED CHANNEL

The constitutive equation for the drift velocity for a multiparticle system in an infinite medium has been studied in the preceding section. We now study the wall effect on the local drift velocity in a channel with uniform cross-sectional area. Under the steady-state condition without phase change ($\Gamma_k = 0$) and with negligible transverse pressure gradient, i.e., $p_c = p_d = p_m(z)$, the axial component of the local momentum equation for phase k can be reduced from Eq. 11 to

$$0 = -\alpha_k \frac{\partial p_m}{\partial z} - \alpha_k M_{\tau k} - \alpha_k \rho_k g_z + M_{ik}, \tag{28}$$

where $M_{\tau k}$ and M_{ik} are the axial forces associated with the transverse stress gradient and the interfacial drag, as shown in Eq. 11. Here we have taken $g_z \geq 0$ such that $v > 0$ when the flow is upward. Consequently we obtain

$$\left.\begin{aligned} M_{ic} &= \alpha_c\left(\rho_c g_z + \frac{\partial p_m}{\partial z}\right) + M_{\tau c}\alpha_c \\ \text{and} \\ M_{id} &= \alpha_d\left(\rho_d g_z + \frac{\partial p_m}{\partial z}\right) + M_{\tau d}\alpha_d. \end{aligned}\right\} \tag{29}$$

However, from the interfacial-force balance, we have

$$M_{ic} + M_{id} = 0. \tag{30}$$

Thus by eliminating the interfacial forces from the above two equations, we get the local z components of the mixture-momentum equation as

$$\frac{\partial p_m}{\partial z} = -\rho_m g_z - M_{\tau m}, \tag{31}$$

where $M_{\tau m}$ is the force associated with mixture transverse stress gradient and given by $M_{\tau m} = \alpha_d M_{\tau d} + (1 - \alpha_d) M_{\tau c}$.

From Eq. 29 and 31, we obtain

$$M_{id} = -\alpha_d[(1 - \alpha_d) g_z(\rho_c - \rho_d) + (M_{\tau m} - M_{\tau d})]. \tag{32}$$

However, inasmuch as the interfacial force M_{id} is related to the drag force by $F_D = M_{id} V_d / \alpha_d$, Eqs. 15 and 32 can be solved for the relative velocity as

$$v_r|v_r| = \frac{8}{3}\frac{r_d}{C_D\rho_c}[(\rho_c - \rho_d)g_z(1 - \alpha_d) + (M_{\tau m} - M_{\tau d})]. \tag{33}$$

By introducing the nondimensional groups

$$\left.\begin{aligned} g^* &\equiv g_z(\rho_c - \rho_d)/(\Delta\rho g) \\ \text{and} \\ M_\tau^* &\equiv (M_{\tau m} - M_{\tau d})/(\Delta\rho g) \end{aligned}\right\}, \tag{34}$$

where $\Delta\rho = |\rho_c - \rho_d|$, we obtain, from Eqs. 18, 19, and 33,

$$C_{D_\infty}(N_{Re_\infty}) = C_D(N_{Re})\left(\frac{v_r}{v_{r_\infty}}\right)^2 \Big/ |g^*(1 - \alpha_d) + M_\tau^*|. \tag{35}$$

By using the same similarity hypothesis as used for systems in infinite media, we can find the expression for the velocity ratio for a channel flow. The results are summarized below:

Undistorted-particle Regime:

$$V_{dj} = |v_{r\infty}|(1 - \alpha_d)[g^*(1 - \alpha_d) + M_\tau^*]\frac{\mu_c}{\mu_m}\frac{1 + \psi(r_d^*)}{1 + \psi(r_d^*)[f(\alpha_d)]^{6/7}}, \tag{36}$$

where $f(\alpha_d) \equiv (\mu_c/\mu_m)|g^*(1 - \alpha_d) + M_\tau^*|^{0.5}$ and $\psi(r_d^*)$ is given by

$$\psi(r_d^*) = \begin{cases} 0.55[(1 + 0.08r_d^{*3})^{4/7} - 1]^{0.75}; & r^* < 34.65; \\ \\ 17.67; & r_d^* \geq 34.65. \end{cases} \tag{37}$$

Distorted-particle Regime:

$$V_{dj} = |v_{r\infty}|(1 - \alpha_d)\frac{\mu_c}{\mu_m}|g^*(1 - \alpha_d) + M_\tau^*|\frac{18.67}{1 + 17.67[f(\alpha_d)]^{6/7}} \tag{38}$$

Churn-turbulent-flow Regime:

$$V_{dj} = \sqrt{2}\left(\frac{g\Delta\rho\sigma}{\rho_c^2}\right)^{1/4}\frac{g^*(1 - \alpha_d) + M_\tau^*}{|g^*(1 - \alpha_d) + M_\tau^*|^{0.75}} \tag{39}$$

If the effect of the wall can be neglected and the flow is vertical, $g^* = 1$ and $M_T^* = 0$; hence, we have approximately

$$V_{dj} = \sqrt{2}\left(\frac{\sigma g \Delta\rho}{\rho_c^2}\right)^{1/4}, \tag{40}$$

The expression for the single-particle terminal velocity $v_{r\infty}$ for the corresponding flow regimes appears in the appendix.

The above expressions indicate that the local drift velocity in the axial direction depends on the difference between the transverse stress gradient of each phase; i.e., $M_T^* = (1 - \alpha_d)(M_{Tc} - M_{Td})/(\Delta\rho g)$. To take this effect into account requires additional information concerning the turbulent structure of both the continuous and dispersed phases.

V. ONE-DIMENSIONAL DRIFT-FLUX MODEL

Averaging over the cross-sectional area is useful for complicated engineering problems involving fluid flow and heat transfer, since field equations can be reduced to quasi-one-dimensional forms. By area averaging, the information on changes of variables in the direction normal to the main flow within a channel is basically lost; therefore, the transfer of momentum and energy between the wall and the fluid should be expressed by empirical correlations or by simplified models. The rational approach to obtain a one-dimensional model is to integrate the three-dimensional model over a cross-sectional area and then to introduce proper mean values.

A simple area average over the cross-sectional area A is defined by

$$\langle F \rangle = \frac{1}{A} \int_A F \, dA, \tag{41}$$

and the void-fraction-weighted mean value is given by

$$\langle\langle F_k \rangle\rangle = \langle \alpha_k F_k \rangle / \langle \alpha_k \rangle. \tag{42}$$

In the subsequent analysis, the density of each phase ρ_d and ρ_c within any cross-sectional area is considered to be uniform, so that $\rho_k = \langle\langle \rho_k \rangle\rangle$. For most practical two-phase flow problems, this assumption is valid since the transverse pressure gradient within a channel is relatively small. The detailed analysis without this approximation appears in Ref. 24. Under the above simplifying assumption, the average mixture density is given by

$$\langle \rho_m \rangle \equiv \langle \alpha_d \rangle \rho_d + (1 - \langle \alpha_d \rangle)\rho_c. \tag{43}$$

The axial component of the weighted mean velocity of phase k is

$$\langle\langle v_k \rangle\rangle = \frac{\langle \alpha_k v_k \rangle}{\langle \alpha_k \rangle} = \frac{\langle j_k \rangle}{\langle \alpha_k \rangle}, \tag{44}$$

where the scalar expression of the velocity corresponds to the axial component of the vector. Then the mixture velocity is defined by

$$\bar{v}_m \equiv \frac{\langle \rho_m v_m \rangle}{\langle \rho_m \rangle} = [\langle \alpha_d \rangle \rho_d \langle\langle v_d \rangle\rangle + (1 - \langle \alpha_d \rangle)\rho_c \langle\langle v_c \rangle\rangle]/\langle \rho_m \rangle, \tag{45}$$

and the volumetric flux is given by

$$\langle j \rangle \equiv \langle j_d \rangle + \langle j_c \rangle = \langle \alpha_d \rangle \langle\langle v_d \rangle\rangle + (1 - \langle \alpha_d \rangle)\langle\langle v_c \rangle\rangle. \tag{46}$$

The mean mixture enthalpy also should be weighted by the density; thus,

$$\bar{h}_m \equiv \frac{\langle \rho_m h_m \rangle}{\langle \rho_m \rangle} = [\langle \alpha_d \rangle \rho_d \langle\langle h_d \rangle\rangle + (1 - \langle \alpha_d \rangle)\rho_c \langle\langle h_c \rangle\rangle]/\langle \rho_m \rangle. \tag{47}$$

The appropriate mean drift velocity is defined by

$$\bar{V}_{dj} \equiv \langle\langle v_d \rangle\rangle - \langle j \rangle = (1 - \langle \alpha_d \rangle)(\langle\langle v_d \rangle\rangle - \langle\langle v_c \rangle\rangle). \tag{48}$$

The experimental determination of the above-defined drift velocity is possible if the volume flow rate of each phase, Q_k, and the mean void fraction $\langle \alpha_d \rangle$ are measured. This is because Eq. 48 can be transformed into

$$\bar{V}_{dj} = \frac{\langle j_d \rangle}{\langle \alpha_d \rangle} - (\langle j_d \rangle + \langle j_c \rangle), \tag{49}$$

where $\langle j_k \rangle$ is given by $\langle j_k \rangle = Q_k/A$. Furthermore, the present definition of the drift velocity can also be used for annular two-phase flows. Under the definitions of various velocity fields we obtain several important relations, such as

$$\left.\begin{aligned} \langle\langle v_d \rangle\rangle &= \bar{v}_m + \frac{\rho_c}{\langle \rho_m \rangle}\bar{V}_{dj}, \\ \langle\langle v_c \rangle\rangle &= \bar{v}_m - \frac{\langle \alpha_d \rangle}{1 - \langle \alpha_d \rangle}\frac{\rho_d}{\langle \rho_m \rangle}\bar{V}_{dj}, \end{aligned}\right\} \tag{50}$$

and

$$\langle j \rangle = \bar{v}_m + \frac{\langle \alpha_d \rangle (\rho_c - \rho_d)}{\langle \rho_m \rangle} \bar{V}_{dj}. \tag{51}$$

In the drift-flux formulation, a problem is solved for $\langle \alpha_d \rangle$ and $\bar{v}_m$ with a given constitutive relation for $\bar{V}_{dj}$. Thus Eq. 50 can be used to recover a solution for the velocity of each phase after a problem is solved.

By area-averaging Eqs. 1-4 and using the various mean values, we obtain:

Mixture Continuity Equation:

$$\frac{\partial \langle \rho_m \rangle}{\partial t} + \frac{\partial}{\partial z}(\langle \rho_m \rangle \bar{v}_m) = 0. \tag{52}$$

Continuity Equation for Dispersed Phase:

$$\frac{\partial \langle \alpha_d \rangle \rho_d}{\partial t} + \frac{\partial}{\partial z}(\langle \alpha_d \rangle \rho_d \bar{v}_m) = \langle \Gamma_d \rangle - \frac{\partial}{\partial z}\left(\frac{\langle \alpha_d \rangle \rho_d \rho_c}{\langle \rho_m \rangle} \bar{V}_{dj} \right). \tag{53}$$

Mixture Momentum Equation:

$$\frac{\partial \langle \rho_m \rangle \bar{v}_m}{\partial t} + \frac{\partial}{\partial z}(\langle \rho_m \rangle \bar{v}_m^2) = -\frac{\partial}{\partial z}\langle p_m \rangle + \frac{\partial}{\partial z}\langle \tau_{zz} + \tau_{zz}^T \rangle - \langle \rho_m \rangle g_z$$

$$- \frac{f_m}{2D}\langle \rho_m \rangle \bar{v}_m |\bar{v}_m| - \frac{\partial}{\partial z}\left[\frac{\langle \alpha_d \rangle \rho_d \rho_c}{(1 - \langle \alpha_d \rangle)\langle \rho_m \rangle} \bar{V}_{dj}^2 \right]$$

$$- \frac{\partial}{\partial z} \sum_k \mathrm{COV}(\alpha_k \rho_k v_k v_k). \tag{54}$$

Mixture Enthalpy-energy Equation:

$$\frac{\partial \langle \rho_m \rangle \bar{h}_m}{\partial t} + \frac{\partial}{\partial z}(\langle \rho_m \rangle \bar{h}_m \bar{v}_m) = -\frac{\partial}{\partial z}\langle q + q^T \rangle + \frac{q''_W \xi_h}{A} - \frac{\partial}{\partial z} \frac{\langle \alpha_d \rangle \rho_d \rho_c}{\langle \rho_m \rangle} \Delta h_{dc} \bar{V}_{dj}$$

$$- \frac{\partial}{\partial z}\left[\frac{\langle \alpha_d \rangle \rho_d \rho_c}{\langle \rho_m \rangle} \Delta h_{dc} \bar{V}_{dj} \right] - \frac{\partial}{\partial z} \sum_k \mathrm{COV}(\alpha_k \rho_k h_k v_k) + \frac{\partial \langle p_m \rangle}{\partial t}$$

$$+ \left[\bar{v}_m + \frac{\langle \alpha_d \rangle (\rho_c - \rho_d)}{\langle \rho_m \rangle} \bar{V}_{dj} \right] \frac{\partial \langle p_m \rangle}{\partial z} + \langle \Phi_m^\mu \rangle. \tag{55}$$

Here $\tau_{zz} + \tau_{zz}^{T}$ denotes the normal components of the stress tensor in the axial direction and Δh_{dc} is the enthalpy difference between phases; thus, $\Delta h_{dc} = \langle\langle h_d \rangle\rangle - \langle\langle h_c \rangle\rangle$. The covariance terms represent the difference between the average of a product and the product of the average of two variables such that $\text{COV}(\alpha_k \rho_k \psi_k v_k) \equiv \langle \alpha_k \rho_k \psi_k (v_k - \langle\langle v_k \rangle\rangle) \rangle$. If the profile of either ψ_k or v_k is flat, then the covariance term reduces to zero. The term represented by $f_m \langle \rho_m \rangle \bar{v}_m |\bar{v}_m|/(2D)$ in Eq. 54 is the two-phase frictional pressure drop. We note here that the effects of the mass, momentum, and energy diffusion associated with the relative motion between phases appear explicitly in the drift-flux formulation, since the convective terms on the left-hand side of the field equations are expressed in terms of the mixture velocity. These effects of diffusions in the present formulation are expressed in terms of the drift velocity of the dispersed phase $\bar{V}_{dj}$. This may be formulated in a functional form as

$$\bar{V}_{dj} = \bar{V}_{dj}(\langle \alpha_d \rangle, \langle p_m \rangle, g_z, \bar{v}_m, \text{etc.}). \tag{56}$$

To take into account the mass transfer across the interfaces, a constitutive equation for $\langle \Gamma_d \rangle$ should also be given. In a functional form, this phase-change constitutive equation may be written as

$$\langle \Gamma_d \rangle = \langle \Gamma_d \rangle \left(\langle \alpha_d \rangle, \langle p_m \rangle, \bar{v}_m, \frac{\partial \langle p_m \rangle}{\partial t}, \text{etc.} \right). \tag{57}$$

The above formulation can be extended to nondispersed two-phase flows, such as an annular flow, provided a proper constitutive relation for a drift velocity of one of the phases is given.

VI. ONE-DIMENSIONAL DRIFT VELOCITY

A. Dispersed Two-phase Flow

To obtain a kinematic constitutive equation for the one-dimensional drift-flux model, we must average the local drift velocity over the channel cross section. The constitutive relation for the local drift velocity V_{dj} in a confined channel was developed in Sec. IV. Now we shall relate this to the mean drift velocity $\bar{V}_{dj}$ defined by Eq. 48.

From Eqs. 42 and 48,

$$\bar{V}_{dj} = \left\langle \frac{\alpha_d (j + V_{dj})}{\langle \alpha_d \rangle} - j \right\rangle = \langle\langle V_{dj} \rangle\rangle + (C_0 - 1)\langle j \rangle, \tag{58}$$

where

$$\langle\langle V_{dj}\rangle\rangle \equiv \langle\alpha_d V_{dj}\rangle/\langle\alpha_d\rangle \tag{59}$$

and

$$C_0 \equiv \frac{\langle\alpha_d j\rangle}{\langle\alpha_d\rangle\langle j\rangle}. \tag{60}$$

The second term on the right-hand side of Eq. 58 is a covariance between the concentration profile and the volumetric flux profile; thus it can also be expressed as $\mathrm{COV}(\alpha_{dj})/\langle\alpha_d\rangle$. The factor C_0, which has been used for bubbly or slug flows by several authors,[10,25,26] is known as a distribution parameter. The inverse of this parameter was also used in the early work of Bankoff.[27] Physically, this effect arises from the fact that the dispersed phase is locally transported with the drift velocity V_{dj} with respect to local volumetric flux j and not to the average volumetric flux $\langle j\rangle$. For example, if the dispersed phase is more concentrated in the higher-flux region, then the mean transport of the dispersed phase is promoted by higher local j.

The value of C_0 can be determined from assumed profiles of the void fraction α_d and total volumetric flux j,[10] or from experimental data.[11] By assuming power-law profiles in a pipe for j and α_d, we have

$$\left.\begin{aligned} j/j_0 &= 1 - (R/R_W)^m; \\ \frac{\alpha_d - \alpha_{dW}}{\alpha_{d0} - \alpha_{dW}} &= 1 - (R/R_W)^n, \end{aligned}\right\} \tag{61}$$

where j_0, α_{d0}, α_{dW}, R, and R_W are, respectively, the value of j and α at the center, the void fraction at the wall, radial distance, and the radius of a pipe. By substituting these profiles into the definition of C_0 given by Eq. 60, we obtain

$$C_0 = 1 + \frac{2}{m + n + 2}\left(1 - \frac{\alpha_{dW}}{\langle\alpha_d\rangle}\right). \tag{62}$$

The distribution parameter based on the above assumed profiles is further discussed in Ref. 11.

Now Eq. 58 can be transformed to

$$\langle\langle v_d\rangle\rangle = \frac{\langle j_d\rangle}{\langle\alpha_d\rangle} = C_0\langle j\rangle + \langle\langle V_{dj}\rangle\rangle, \tag{63}$$

where $\langle\langle v_d \rangle\rangle$ and $\langle j \rangle$ are easily obtainable parameters in experiments, particularly under an adiabatic condition. Therefore, this equation suggests a plot of the mean velocity $\langle\langle v_d \rangle\rangle$ versus the average volumetric flux $\langle j \rangle$. Various experimental data using this mean velocity-flux plane are in Figs. 6-12. If the concentration profile is uniform across the channel, then the value of the distribution parameter is equal to unity. In addition, if the effect of the local drift $\langle\langle V_{dj} \rangle\rangle$ is negligibly small, then the flow becomes essentially homogeneous. In this case, the relation between the mean velocity and flux reduces to a straight line through the origin at an angle of 45°. The deviation of the experimental data from this homogeneous flow line shows the magnitude of the drift of the dispersed phase with respect to the volume center of the mixture.

An important characteristic of such a plot is that, for two-phase flow regimes with fully developed void and velocity profiles, the data points cluster around a straight line (see Figs. 6-12). This trend is particularly pronounced when the local drift velocity is constant or negligibly small. Hence, for a given flow regime, the value of the distribution parameter C_0 may be obtained from the slope of these lines, whereas the intercept of this line with the mean velocity axis can be interpreted as the weighted mean local drift velocity, $\langle\langle V_{dj} \rangle\rangle$. The extensive study by Zuber et al.[11] shows that C_0 depends on pressure, channel geometry, and perhaps flow rate. An important effect of subcooled boiling and developing void profile on the distribution parameter has also been noted by Hancox and Nicoll.[33]

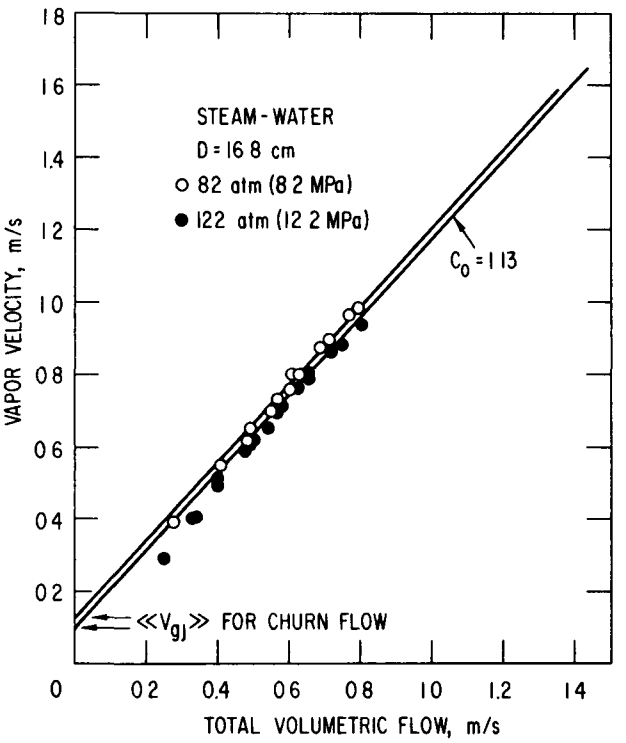

Fig. 6. Experimental Data for High-pressure System.[28] ANL Neg. No. 900-77-187 Rev. 1.

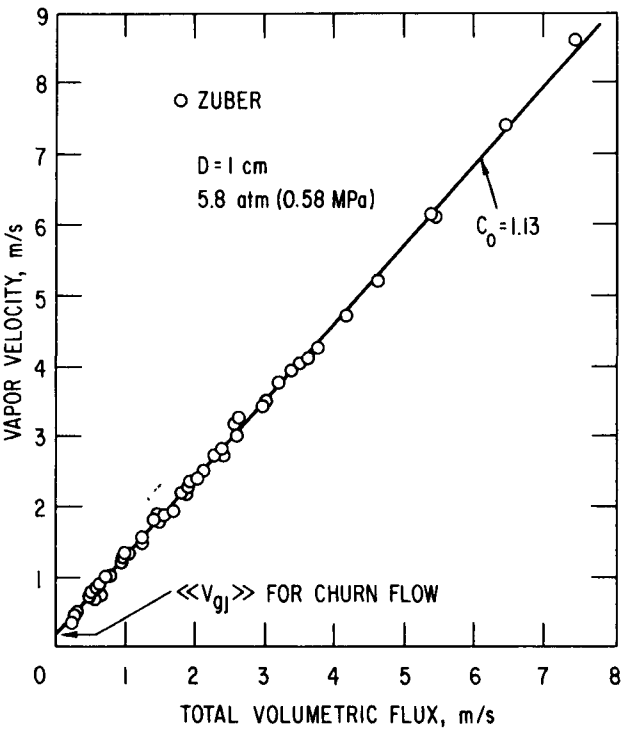

Fig. 7. Freon-22 Data in Boiling Flow.[11] ANL Neg. No. 900-77-181 Rev. 1.

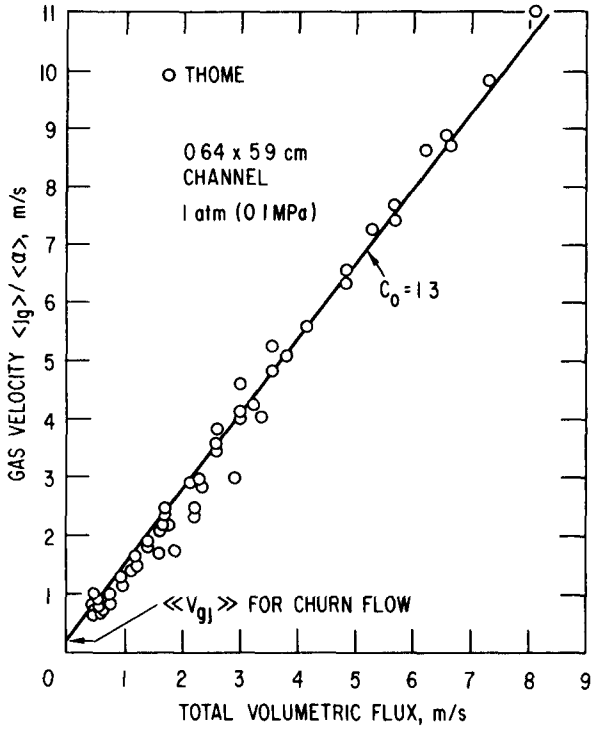

Fig. 8. Fully Developed N_2–NaK Flow.[29] ANL Neg. No. 900–77–177 Rev. 1.

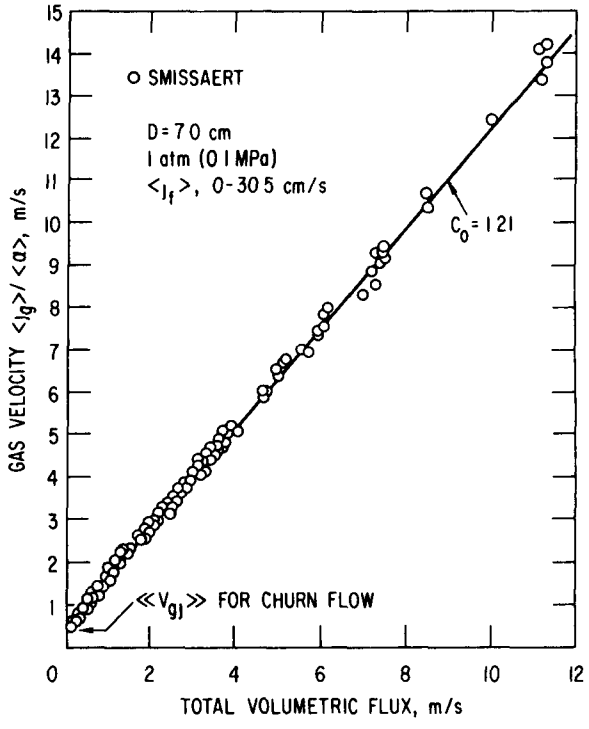

Fig. 9. Fully Developed Air–Water Flow Data.[30] ANL Neg. No. 900–77–182 Rev. 1.

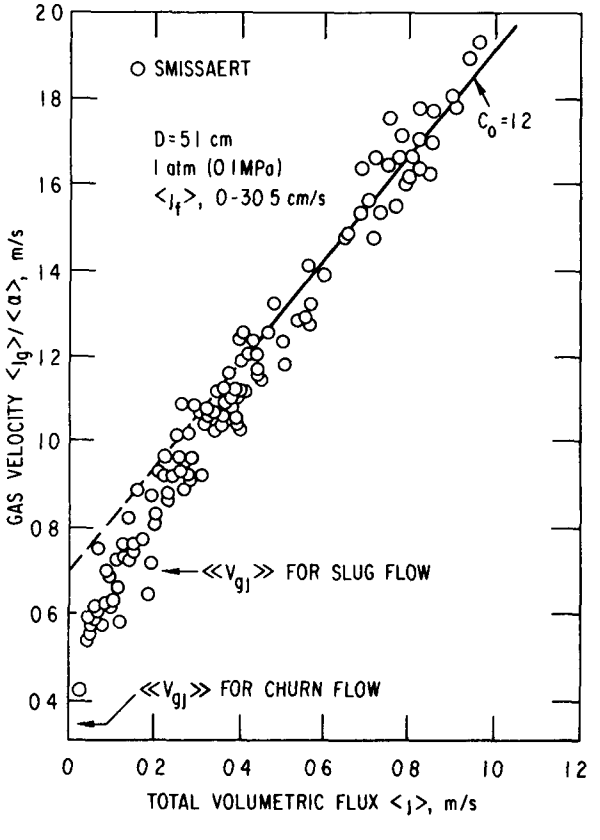

Fig. 10. Fully Developed N_2–Mercury Flow Data.[30] ANL Neg. No. 900–77–176 Rev. 1.

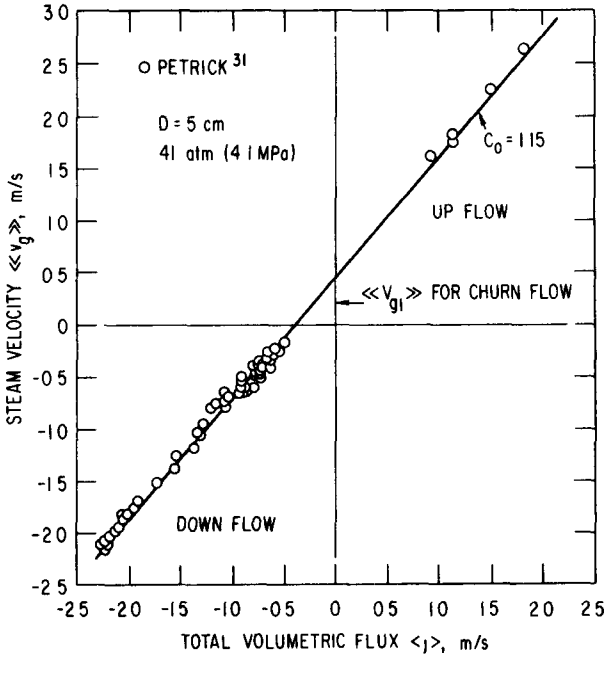

Fig. 11. Experimental Data for Cocurrent Upflow and Cocurrent Downflow of Steam–Water System. ANL Neg. No. 900–77–180 Rev. 1.

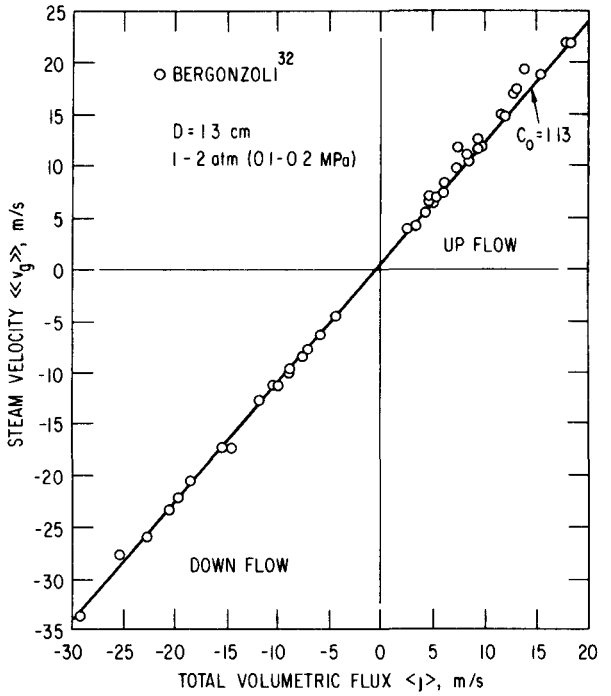

Fig. 12

Experimental Data for Cocurrent Upflow and Cocurrent Downflow of Heated Santowax-R System. ANL Neg. No. 900-77-185 Rev. 2.

In the present study, a simple correlation for the distribution parameter in bubbly-flow regime has been developed along the above studies. First, by considering a fully developed bubbly flow, we assumed that C_0 depends on the density ratio ρ_g/ρ_f and on the Reynolds number based on liquid properties, GD/μ_f, where G, D, and μ_f are the total mass flow rate, hydraulic diameter, and the viscosity of the liquid, respectively. Hence,

$$C_0 = C_0\left(\frac{\rho_g}{\rho_f}, \frac{GD}{\mu_f}\right). \tag{64}$$

A single-phase turbulent-flow profile and the ratio of the maximum velocity to mean velocity give a theoretical limiting value of C_0 at $\alpha \to 0$ and $\rho_g/\rho_f \to 0$, since in this case all the bubbles should be concentrated at the central region. Thus from the experimental data of Nikuradse[34] for a round tube, which gives the ratio of the maximum to mean velocity, we have

$$C_\infty = \lim \frac{\langle \alpha j \rangle}{\langle \alpha \rangle \langle j \rangle} = \frac{\langle \alpha \rangle j_0}{\langle \alpha \rangle \langle j \rangle} = 1.393 - 0.0155\, \ell n\left(\frac{GD}{\mu_f}\right) \tag{65}$$

as $\alpha \to 0$ and $\rho_g/\rho_f \to 0$ (see Fig. 13). On the other hand, as the density ratio approaches the unity, the distribution parameter C_0 should also become unity. Thus,

$$C_0 \to 1 \tag{66}$$

as $\rho_g/\rho_f \to 1$.

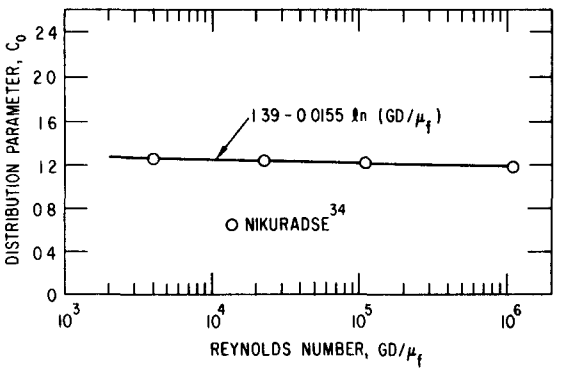

Fig. 13

Limiting Value of Distribution Parameter C_0 at Zero Void Fraction and $\rho_g/\rho_f \to 0$ Based on Single-phase Turbulent-flow Profile. ANL Neg. No. 900-77-178 Rev. 1.

Based on these limits and various experimental data in a fully developed flow, the distribution parameter can be given approximately by

$$C_0 = C_\infty - (C_\infty - 1)\sqrt{\rho_g/\rho_f}, \tag{67}$$

where the density group scales the inertia effects of each phase in a transverse void distribution. Physically, Eq. 67 models the tendency of the lighter phase to migrate into a higher-velocity regime, thus resulting in a higher void concentration in the central regime.[27] For a laminar flow, C_∞ is 2, but, due to the large velocity gradient, C_0 is very sensitive to $\langle\alpha\rangle$ at low void fractions.

Over a wide range of Reynolds number, GD/μ_f, Eq. 65 can be approximated by $C_\infty \simeq 1.2$ for a flow in a round tube. On the other hand, for a rectangular channel, the experimental data show this value to be approximately 1.35. Thus, for a fully developed turbulent bubbly flow,

$$C_0 \simeq \begin{cases} 1.2 - 0.2\sqrt{\rho_g/\rho_f}: & \text{round tube;} \\ 1.35 - 0.35\sqrt{\rho_g/\rho_f}: & \text{rectangular channel.} \end{cases} \tag{68}$$

Figures 14 and 15 compare the above correlation with various experimental data. Each point in the figures represents anywhere from five to 150 data points. For example, the original experimental data of Smissaert,[30] shown in Fig. 9, are presented by a single point in Fig. 14. Each point in Fig. 9 can be used to obtain a corresponding value for C_0 by using the existing correlation for the mean local drift velocity $\langle\langle V_{dj}\rangle\rangle$. However, in view of the strong linear relation between the mean velocity of the dispersed phase and the total flux, the average value of C_0 obtained by linear fitting has been used in Figs. 14 and 15.

In the velocity-flux plane (see Figs. 11 and 12), three operational modes can be easily identified. In the first quadrant, the flow is basically cocurrent upward; therefore both the liquid and vapor phases flow in an upward direction. Examples of this mode are shown in Figs. 6-10. In the second quadrant, the

vapor phase is moving upward; however, there is a net downward flow of mixture. Consequently, the flow is countercurrent. The cocurrent downflow operation should appear in the third quadrant of the velocity-flux plane, as shown in Figs. 11 and 12. These data indicate that the basic characteristic described by Eq. 63 is valid for both cocurrent up and down flows with an identical value for the distribution parameter C_0. This fact demonstrates the usefulness of correlating the drift velocity in terms of the mean local drift velocity $\langle\langle V_{dj} \rangle\rangle$ and C_0.

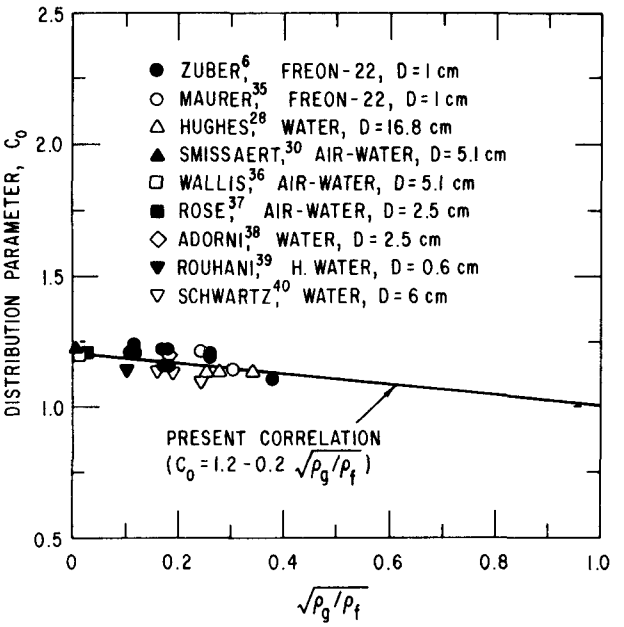

Fig. 14. Distribution Parameter for Fully Developed Flow in a Round Tube. ANL Neg. No. 900-77-173 Rev. 1.

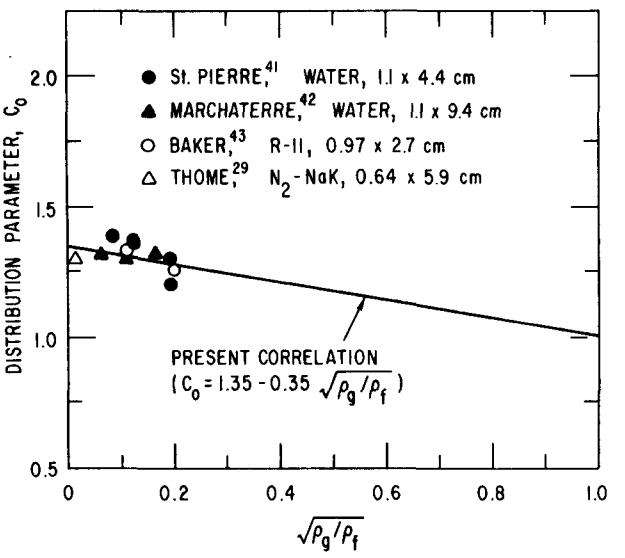

Fig. 15. Distribution Parameter for Fully Developed Flow in a Rectangular Channel. ANL Neg. No. 900-77-184 Rev. 1.

In two-phase systems with heat addition, the change of void profiles from concave to convex can occur as illustrated in Figs. 16 and 17. The concave void-fraction profile is caused by the wall nucleation and delayed transverse migration of bubbles toward the center of a channel. Under these conditions, most of the bubbles are initially located near the nucleating wall. The concave profile is particularly pronounced in the subcooled boiling regime, because here only the wall-boundary layer is heated above the saturation temperature and the core liquid is subcooled. This temperature profile will induce collapses of migrating bubbles in the core region and resultant latent heat transport from the wall to the subcooled liquid. However, a similar concave profile can also be obtained by injecting gas into flowing liquid through a porous tube wall.[37]

In the region in which voids are still concentrated close to the wall, the mean velocity of vapor can be less than the mean velocity of liquid, because the bulk of liquid moves with the high core velocity. Hence, in this region,

the data should fall below the line for a fully developed two-phase flow. This is illustrated in Figs. 18-20. If the data fall below the homogeneous line, the value of C_0 should be less then unity. However, as more and more vapor is

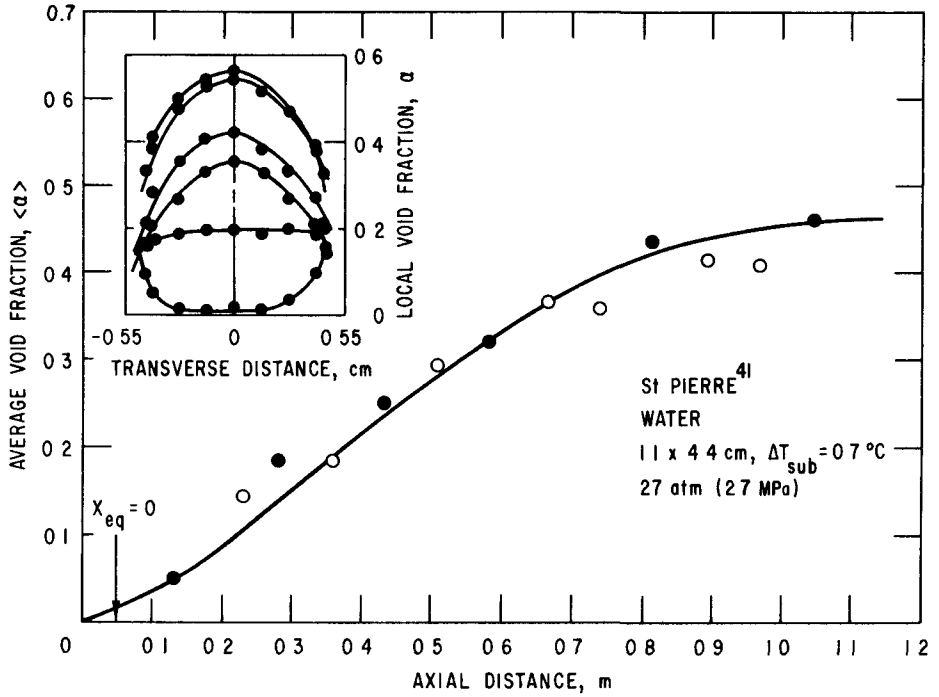

Fig. 16. Axial Void Distribution with Corresponding Void Profiles at Various Stations for Steam-Water Experiment in Rectangular Channel. ANL Neg. No. 900-77-172 Rev. 1.

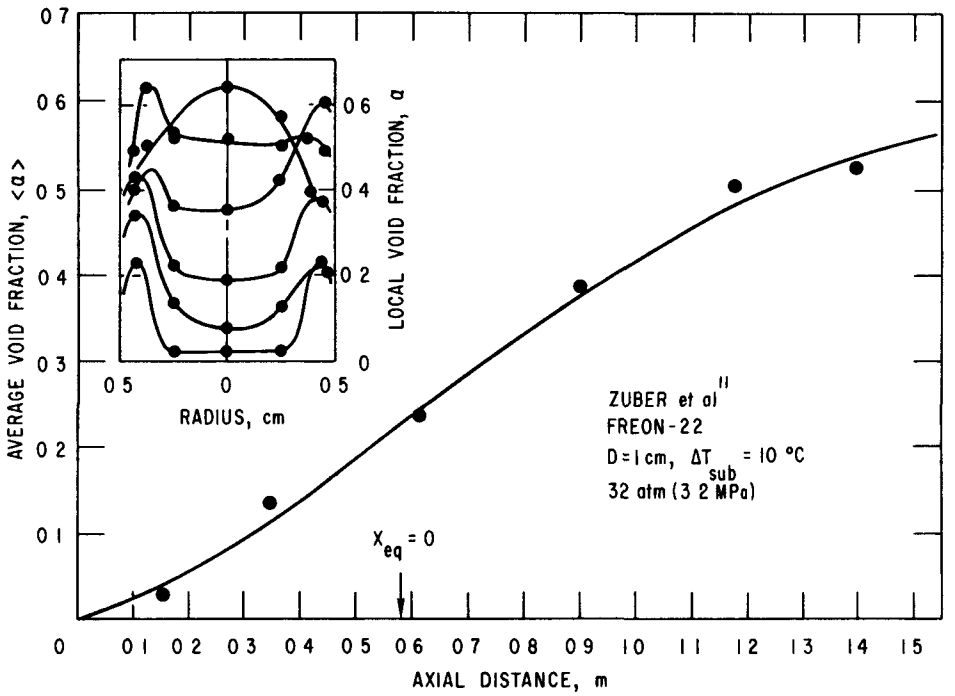

Fig. 17. Axial Void Distribution with Corresponding Void Profiles at Various Stations for Freon-22 Experiment in Round Tube. ANL Neg. No. 900-77-183 Rev. 1.

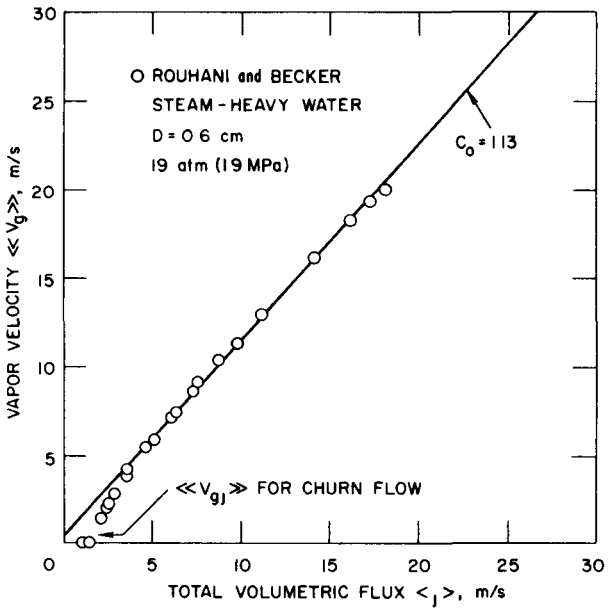

Fig. 18

Experimental Data of Rouhani and Becker[39] in Round Tube and Effect of Developing Flow due to Boiling. ANL Neg. No. 900-77-179 Rev. 1.

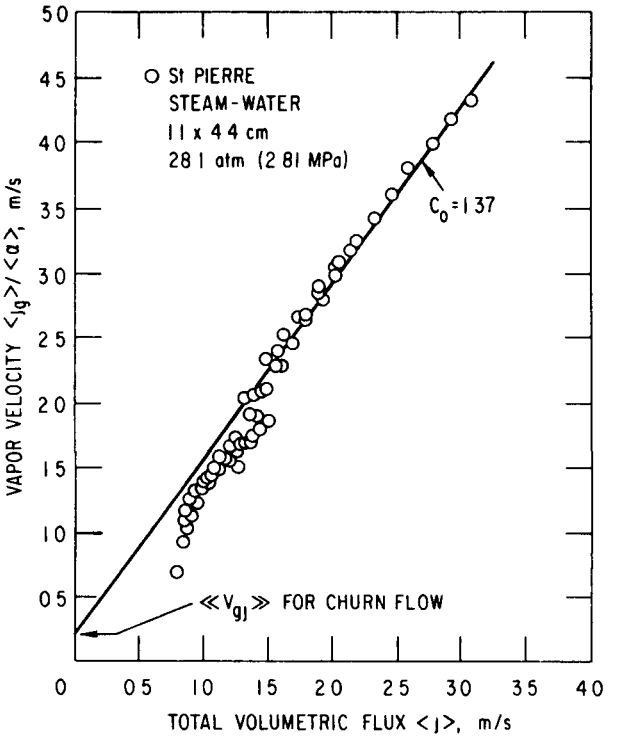

Fig. 19

Experimental Data of St. Pierre[41] in Rectangular Flow and Effect of Developing Flow due to Boiling. ANL Neg. No. 900-77-174 Rev. 1.

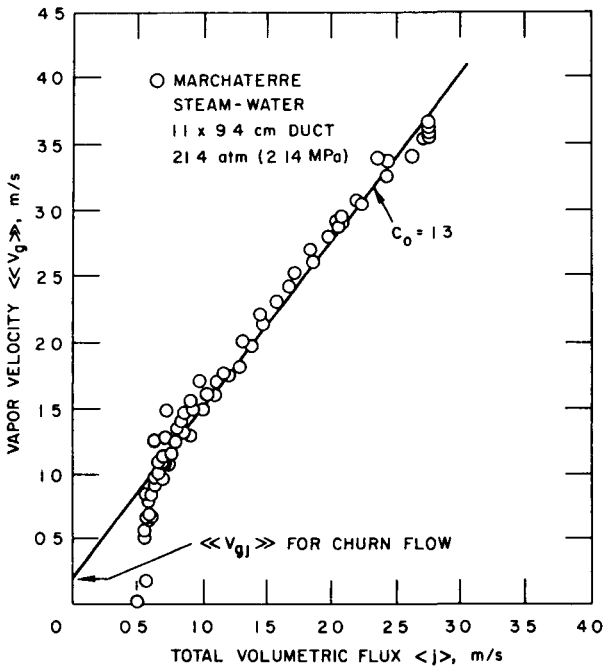

Fig. 20

Experimental Data of Marchaterre[42] in Rectangular Duct and Effect of Developing Flow due to Boiling. ANL Neg. No. 900-77-175 Rev. 1.

generated along the channel, the void-fraction profile changes from concave to convex and becomes fully developed. This trend can easily be seen in Figs. 18-20, in which the data approach the fully developed flow line from below in the bulk boiling regime.

For a flow with generation of void at the wall due to either nucleation or gas injection, the distribution parameter C_0 should have a near-zero value at the beginning of the two-phase flow region. This can be also seen from the definition of C_0 in Eq. 60. Hence, we have

$$\lim_{\langle\alpha\rangle\to 0} C_0 = \lim \frac{\langle\alpha j\rangle}{\langle\alpha\rangle\langle j\rangle} = \frac{\langle\alpha\rangle j_w}{\langle\alpha\rangle\langle j\rangle} = 0 \quad \text{for} \quad \Gamma_g > 0. \tag{69}$$

With the increase in the cross-sectional mean void fraction, the peak of the local void fraction moves from the near-wall region to the central region, as shown in Figs. 16 and 17. This will lead to the increase in the value of C_0 as the void profile develops.

In view of the basic characteristic described above and various experimental data,[11,35,41,42] the following simple correlation is proposed:

$$C_0 = [C_\infty - (C_\infty - 1)\sqrt{\rho_g/\rho_f}](1 - e^{-18\langle\alpha\rangle}). \tag{70}$$

This expression indicates the significance of the developing void profile in the region given by $0 < \langle\alpha\rangle < 0.25$; beyond this region, the value of C_0 approaches rapidly to that for a fully developed flow (see Fig. 21). Hence, for $\Gamma_g > 0$, we obtain

$$C_0 = \begin{cases} (1.2 - 0.2\sqrt{\rho_g/\rho_f})(1 - e^{-18\langle\alpha\rangle}); & \text{round tube;} \\ \\ (1.35 - 0.35\sqrt{\rho_g/\rho_f})(1 - e^{-18\langle\alpha\rangle}); & \text{rectangular channel.} \end{cases} \tag{71}$$

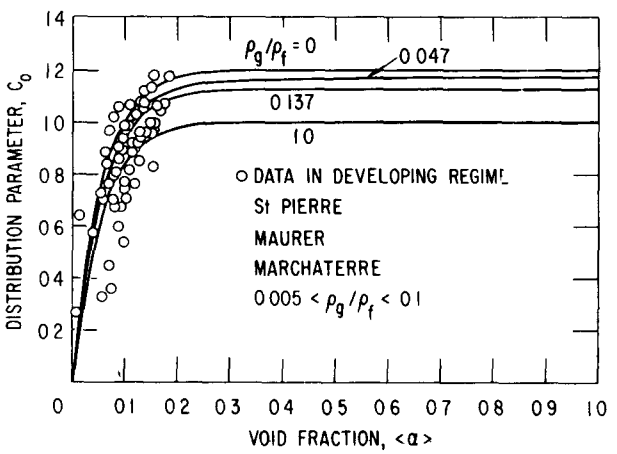

Fig. 21

Distribution Parameter in Developing Flow due to Boiling. (Data for the rectangular duct have been modified by a factor of 1.2/1.35 to obtain corresponding data for a round tube.) ANL Neg. No. 900-77-186 Rev. 1.

For most droplet or particulate flows in the turbulent regime, the volumetric flux profile is quite flat due to the turbulent mixing and particle slips near the wall, which increase the volumetric flux. The concentration

of dispersed phase also tends to be uniform, except for weak peaking near the core of the flow. Because of these profiles for j and α_d, the value of the distribution parameter C_0 is expected to be close to unity ($1.0 \leq C_0 \leq 1.1$). Thus, by assuming that the covariance terms are negligibly small for droplet or particulate flows, we have

$$\bar{V}_{dj} \simeq \langle\langle V_{dj} \rangle\rangle, \tag{72}$$

in which case the local slip becomes important.

The calculation of $\langle\langle V_{dj} \rangle\rangle$ based on the local constitutive equations is the integral transformation, Eq. 59; thus it will require additional information on the void profile[44]. Since this profile is not known in general, we make the following simplifying approximations. The average drift velocity $\langle\langle V_{dj} \rangle\rangle$ due to the local slip can be predicted by the same expression as the local constitutive relations given in Ref. 44, provided the local void fraction α_d and the nondimensional difference of the stress gradient are replaced by average values. These approximations are good for flows with a relatively flat void-fraction profile; also, they can be considered acceptable from the overall simplicity of the one-dimensional model.

For a fully developed vertical flow, the stress distribution in the fluid and in the dispersed phase should be similar; thus the effect of shear gradient on the mean local drift velocity can be neglected. Under these conditions we obtain the following results:

Undistorted-particle Regime:

$$\bar{V}_{dj} = (C_0 - 1)\langle j \rangle + \frac{10.8\mu_c}{\rho_c r_d} \frac{\mu_c}{\langle \mu_m \rangle}(1 - \langle \alpha_d \rangle)^2 \frac{\psi^{4/3}(1 + \psi)}{1 + \psi \left[\frac{\mu_c}{\langle \mu_m \rangle}(1 - \langle \alpha_d \rangle)^{0.5}\right]^{6/7}} \frac{\rho_c - \rho_d}{\Delta\rho}, \tag{73}$$

where $\psi(r_d^*) = 0.55[(1 + 0.08 r_d^{*3})^{4/7} - 1]^{0.75}$ for $r_d^* < 34.65$ and $\psi(r_d^*) = 17.67$ for $r_d^* \geq 34.65$. The limiting case of the undistorted-particle regime is the Stokes regime in which the mean drift velocity reduces to

$$\bar{V}_{dj} = (C_0 - 1)\langle j \rangle + \tfrac{2}{9} r_d^2 \frac{g\Delta\rho}{\mu_c}(1 - \langle \alpha_d \rangle)^2 \frac{\mu_c}{\langle \mu_m \rangle} \frac{\rho_c - \rho_d}{\Delta\rho}. \tag{74}$$

Distorted-particle Regime ($1.75 \leq n \leq 2.25$):

$$\bar{V}_{dj} = (C_0 - 1)\langle j \rangle + \sqrt{2}\left(\frac{\sigma g \Delta\rho}{\rho_c^2}\right)^{1/4}(1 - \langle \alpha_d \rangle)^n \frac{\rho_c - \rho_d}{\Delta\rho}. \tag{75}$$

Here the value of n depends on the viscosities as seen in Eq. 25.

Churn-turbulent-flow Regime:

$$\bar{V}_{dj} = (C_0 - 1)\langle j \rangle + \sqrt{2}\left(\frac{\sigma g \Delta\rho}{\rho_c^2}\right)^{1/4} \frac{\rho_c - \rho_d}{\Delta\rho}. \tag{76}$$

Here the mean mixture viscosity[44] is given by

$$\frac{\langle \mu_m \rangle}{\mu_c} = \left(1 - \frac{\langle \alpha_d \rangle}{\alpha_{dm}}\right)^{-2.5\alpha_{dm}(\mu_d + 0.4\mu_c)/(\mu_d + \mu_c)}. \tag{77}$$

The value of maximum packing, $\alpha_{dm} = 0.62$, is recommended for solid particle-fluid systems, although it can range from 0.5 to 0.74. However, for a bubbly flow, the theoretical value of α_{dm} can be much higher. If we consider the standard range of interest of void fraction in bubbly flow, α_{dm} may be approximated by $\alpha_{dm} = 1$. Hence, for a bubbly flow, the mixture viscosity becomes

$$\frac{\langle \mu_m \rangle}{\mu_c} = \frac{1}{1 - \langle \alpha_d \rangle}. \tag{78}$$

On the other hand, for a particulate flow with a low particle concentration, i.e., $\langle \alpha_d \rangle \ll 1$, $\langle \mu_m \rangle$ can be approximated by

$$\frac{\langle \mu_m \rangle}{\mu_c} = (1 - \langle \alpha_d \rangle)^{-2.6}. \tag{79}$$

In a horizontal flow with a complete suspension of the dispersed phase, the transverse mixing, which keeps the particles suspended, can significantly influence the stress gradient of each phase; thus the stress gradient effect may not be neglected. However, in view of the present state of the art, the assumption $\langle\langle V_{dj} \rangle\rangle \simeq 0$ may be used as a first-order approximation, particularly in high-flux flows.

For high-flux flows, the effect of the local drift $\langle\langle V_{dj} \rangle\rangle$ on the mean drift velocity is small in comparison with the covariance term $(C_0 - 1)\langle j \rangle$. Thus, by neglecting the former, we have

$$\bar{V}_{dj} = \frac{(C_0 - 1)\langle \rho_m \rangle \bar{v}_m}{\langle \rho_m \rangle - (C_0 - 1)\langle \alpha_d \rangle (\rho_c - \rho_d)}. \tag{80}$$

For bubbly flows, the above equation imposes a condition on applicable void-fraction ranges; thus we should have $\langle \rho_m \rangle > (C_0 - 1)\langle \alpha_d \rangle (\rho_c - \rho_d)$. Here a simple criterion for the boundary between the high- and low-flux flow can be obtained by taking the ratio of the total volumetric flux and the terminal velocity. If this ratio is more than 10, the flow can be considered a high-flux flow.

The other limiting case of the dispersed two-phase flow in a confined channel is slug flow. When the volume of a bubble is very large, the shape of the bubble is significantly deformed to fit the channel geometry. The diameters of the bubbles become approximately that of the pipe with a thin liquid film separating the bubbles from the wall. The bubbles have the bullet form with a cap-shaped nose. The motion of these bubbles in relatively inviscid fluids can be studied by using a potential flow analysis around a sphere,[45] and the result is shown to agree with experimental data. Thus,

$$\overline{V}_{dj} = 0.2\langle j \rangle + 0.35\left(\frac{gD\Delta\rho}{\rho_c}\right)^{1/2}, \tag{81}$$

which was originally proposed by Niklin et al.[25] and Neal.[26]

B. Annular Two-phase Flow

In annular two-phase flows, the relative motions between phases are governed by the interfacial geometry, the body-force field, and the interfacial momentum transfer. The constitutive equation for the vapor-drift velocity in annular two-phase flows has been developed by taking into account those macroscopic effects of the structured two-phase flows.[12] Assuming steady-state adiabatic two-phase annular flow with constant single-phase properties, we have the following one-dimensional momentum equations for each phase:

$$-\left(\frac{dp_m}{dz} + \rho_g g_z\right) = \frac{\tau_i P_i}{\langle\alpha\rangle A} \tag{82}$$

and

$$-\left(\frac{dp_m}{dz} + \rho_f g_z\right) = \frac{P_{wf}\tau_{wf}}{A(1 - \langle\alpha\rangle)} - \frac{\tau_i P_i}{A(1 - \langle\alpha\rangle)}, \tag{83}$$

where τ_i, τ_{wf}, P_i, and P_{wf} are the interfacial shear, wall shear, interfacial wetted perimeter, and wall wetted perimeter, respectively. The hydraulic diameter and the ratio of wetted perimeters are defined by $D \equiv 4A/P_{wf}$ and $\xi \equiv P_i/P_{wf}$. By assuming that the film thickness δ is small compared with D, we have $4\delta/D \simeq 1 - \langle\alpha\rangle$. On the other hand, for an annular flow in a pipe, ξ reduces to $\sqrt{\alpha}$.

The wall shear can be expressed through the friction factor with a gravity-correction term by $\tau_{wf} = f_{wf}\rho_f\langle\langle v_f\rangle\rangle|\langle\langle v_f\rangle\rangle|/2 - \Delta\rho g_z\delta/3$, where f_{wf} can be given by the standard friction-factor correlation: $f_{wf} = 16/Re_f$ for laminar film flows and $f_{wf} = 0.0791Re_f^{-0.25}$ for turbulent flows. Here the liquid-film Reynolds number is given by $Re_f = \rho_f|\langle j_f\rangle|D/\mu_f$. Similarly, the interfacial shear can be expressed as $\tau_i = f_i\rho_g|\bar{v}_r|\bar{v}_r/2$ with the interfacial friction factor given by $f_i = 0.005[1 + 75(1 - \langle\alpha\rangle)]$ for rough wavy films.[46]

By definition, the vapor-drift velocity is related to v_r, i.e., $\bar{V}_{gj} = (1 - \langle\alpha\rangle)\bar{v}_r$; hence, by eliminating the pressure gradient from the momentum equations, we obtain for a laminar film

$$\bar{V}_{gj} = \pm\left[\frac{16\langle\alpha\rangle}{\rho_g f_i \xi}\left|\frac{\mu_f\langle j_f\rangle}{D} + \frac{\Delta\rho g_z D(1 - \langle\alpha\rangle)^3}{48}\right|\right]^{1/2} \tag{84}$$

and for a turbulent film

$$\bar{V}_{gj} = \pm\left[\frac{\langle\alpha\rangle(1 - \langle\alpha\rangle)^3 D}{\rho_g f_i \xi}\left|\frac{0.005\rho_f\langle j_f\rangle|\langle j_f\rangle|}{D(1 - \langle\alpha\rangle)^3} + \tfrac{1}{3}\Delta\rho g_z\right|\right]^{1/2}. \tag{85}$$

Here the negative root is taken when the term within the absolute signs becomes negative. The drift velocity in the form expressed by Eqs. 84 and 85 is convenient for use in analyzing steady-state adiabatic or thermal-equilibrium flows, since in these cases the value of $\langle j_f \rangle$ can be easily obtained.

In a general drift-flux-model formulation, $\bar{V}_{gj}$ should be expressed in terms of the mixture velocity $\bar{v}_m$ rather than $\langle j_f \rangle$, as $\bar{v}_m$ is the velocity used in the formulation. From the definition, we have

$$\langle j_f \rangle = (1 - \langle \alpha \rangle)\bar{v}_m - \frac{\langle \alpha \rangle \rho_g}{\langle \rho_m \rangle} \bar{V}_{gj}. \tag{86}$$

By substituting Eq. 86 into Eq. 84, we obtain for a laminar film

$$\bar{V}_{gj} = \pm \frac{8\mu_f \langle \alpha \rangle^2}{\langle \rho_m \rangle D f_i \xi} \left\{ -1 + \left(1 + \frac{f_i D \langle \rho_m \rangle^2 (1 - \langle \alpha \rangle) \xi}{4\mu_f \langle \alpha \rangle^3 \rho_g} \left| \bar{v}_m + \frac{\Delta \rho g_z D^2 (1 - \langle \alpha \rangle)^2}{48\mu_f} \right| \right)^{1/2} \right\}, \tag{87}$$

which is valid for the laminar range given by

$$\frac{(1 - \langle \alpha \rangle)\langle \rho_m \rangle \bar{v}_m - \langle \rho_m \rangle \langle j_f \rangle_{tr}}{\langle \alpha \rangle \rho_g} \leq \bar{V}_{gj} \leq \frac{(1 - \langle \alpha \rangle)\langle \rho_m \rangle \bar{v}_m + \langle \rho_m \rangle \langle j_f \rangle_{tr}}{\langle \alpha \rangle \rho_g}. \tag{88}$$

Here the laminar turbulent-transition volumetric flow is defined by

$$\langle j_f \rangle_{tr} = 3200\mu_f / \rho_f D.$$

The negative root of Eq. 87 applies when the term within the absolute signs becomes negative. It is easy to show that, for $\bar{V}_{gj} \leq (1 - \langle \alpha \rangle)\langle \rho_m \rangle \bar{v}_m / (\langle \alpha \rangle \rho_g)$, the flow is cocurrent upward, whereas, for $\bar{V}_{gj}$ larger than the above limit, the liquid flow is downward.

The solution for the case of turbulent film flow is somewhat more complicated. For convenience, let us introduce the following parameters:

$$\left.\begin{aligned} a &\equiv \frac{f_i \xi \rho_g}{0.005 \langle \alpha \rangle \rho_f (1 - \langle \alpha \rangle)^2}; \\ b &\equiv \frac{\langle \alpha \rangle \rho_g}{\langle \rho_m \rangle (1 - \langle \alpha \rangle)}; \\ c &\equiv \frac{\Delta \rho_g D (1 - \langle \alpha \rangle)}{0.015 \rho_f}. \end{aligned}\right\} \tag{89}$$

Then, for upward liquid flow, we have

$$\bar{V}_{gj} = \begin{cases} \dfrac{-b\bar{v}_m + [a\bar{v}_m^2 + (a - b^2)c]^{1/2}}{(a - b^2)} & \text{if } a - b^2 \neq 0 \\ (\bar{v}_m^2 + c)/2b\bar{v}_m & \text{if } a - b^2 = 0, \end{cases} \tag{90}$$

which applies under the condition $\bar{v}_m \geq \sqrt{cb^2/a}$. However, in the transition regime given by $-\sqrt{c} \leq \bar{v}_m < \sqrt{cb^2/a}$, where the liquid film flow is downward with upward interfacial shear forces on the film, the vapor-drift velocity becomes

$$\bar{V}_{gj} = \frac{b\bar{v}_m + [-a\bar{v}_m^2 + (a + b^2)c]^{1/2}}{a + b^2}. \tag{91}$$

In the range of $\bar{v}_m$ given by $\bar{v}_m \leq -\sqrt{c}$,

$$\bar{V}_{gj} = \frac{-b\bar{v}_m - [a\bar{v}_m^2 - c(a - b^2)]^{1/2}}{a - b^2}, \tag{92}$$

which applies to the cocurrent downward flow.

The above solution can be applied only if the following turbulent-flow criterion is satisfied:

$$\left.\begin{array}{l} \bar{V}_{gj} \leq [(1 - \langle\alpha\rangle)\langle\rho_m\rangle\bar{v}_m - \langle\rho_m\rangle\langle j_f\rangle_{tr}]/\langle\alpha\rangle\rho_g \\ \text{or} \\ \bar{V}_{gj} \geq [1 - \langle\alpha\rangle)\langle\rho_m\rangle\bar{v}_m + \langle\rho_m\rangle\langle j_f\rangle_{tr}]/\langle\alpha\rangle\rho_g \end{array}\right\}. \tag{93}$$

These results do not have a very simple form for a turbulent film. However, if the absolute value of the mixture velocity is large, so that the flow is essentially cocurrent and the gravity effect is small, then the turbulent solution can be approximated by the simple form

$$\bar{V}_{gj} = \frac{(1 - \langle\alpha\rangle)\bar{v}_m}{\dfrac{\langle\alpha\rangle\rho_g}{\langle\rho_m\rangle} + \left\{\dfrac{\xi\rho_g[1 + 75(1 - \langle\alpha\rangle)]}{\langle\alpha\rangle\rho_f}\right\}^{1/2}}. \tag{94}$$

Equation 94 for the drift velocity can be transformed to obtain the slip ratio v_g/v_f under the simplifying assumption that the average liquid velocity is much smaller than the vapor velocity. Then we have

$$\frac{\langle\langle v_g\rangle\rangle}{\langle\langle v_f\rangle\rangle} = \sqrt{\frac{\rho_f}{\rho_g}}\left[\frac{\sqrt{\langle\alpha\rangle}}{1 + 75(1 - \langle\alpha\rangle)}\right]^{1/2} \tag{95}$$

for an annular flow in a pipe for which $\xi = \sqrt{\langle\alpha\rangle}$. The above expression for slip ratio is similar to that obtained by Fauske,[47] namely, $\langle\langle v_g\rangle\rangle/\langle\langle v_f\rangle\rangle = (\rho_f/\rho_g)^{1/2}$, which has no dependence on the void fraction. The factor that takes the void fraction into account in Eq. 94 varies roughly from 0.24 to 1 for the range $0.8 < \alpha < 1$. Therefore, for a turbulent film, the Fauske correlation should give reasonably accurate results at high void fractions.

The predicted vapor-drift velocity was compared to data from various experiments[48-50] under steady-state conditions as shown in Fig. 22. The three sets of data considered constitute about 350 data points for annular and drop-annular flow regimes. Theoretical predictions are within about ±30% of the experimental values over a wide range of vapor-drift velocity between 20 and 250 cm/s. A quite uniform distribution of the data can be attributed to the uncertainty in the determination of void fraction in the above experiments.

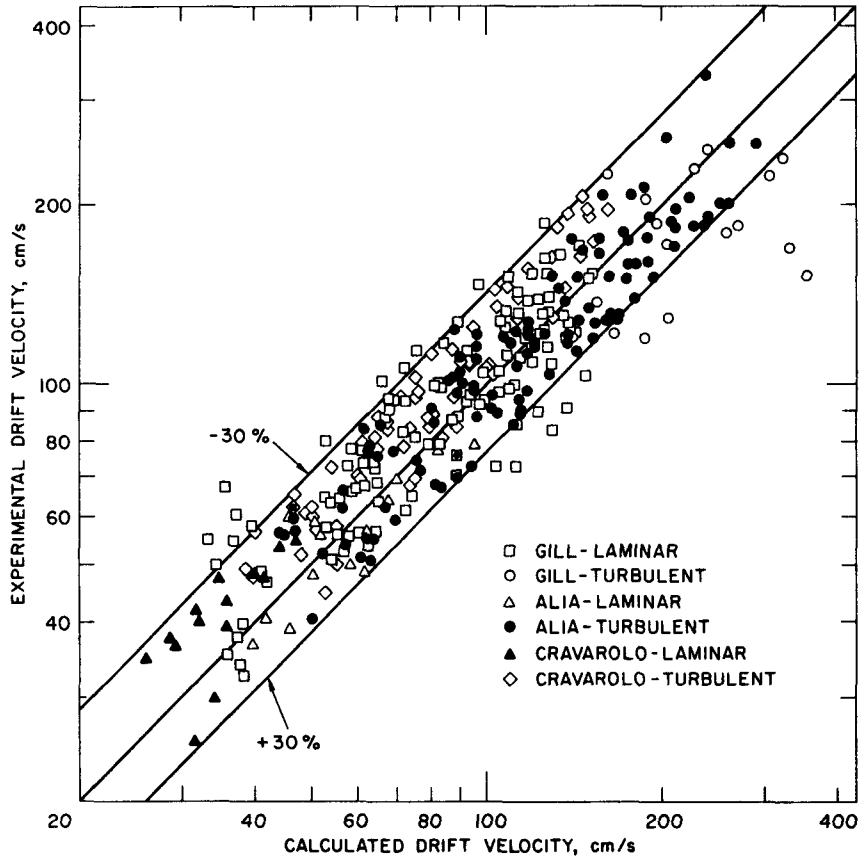

Fig. 22. Comparison of Annular-flow Correlation with Experimental Data. ANL Neg. No. 900-5768.

We note here that these data include a considerable number of points taken in the drop-annular flow regime at moderate rates of gas flow. This indicates that the present vapor-drift-velocity correlation can be used both for ideal annular flows without entrainment as well as for annular mist flows with moderate to low entrainment. However, as the amount of liquid entrained in the gas core becomes large at high rates of gas flow,[46,51] the measured vapor-drift velocity starts to depart considerably from the predicted values and the present analysis overpredicts these values.

The drift-velocity correlation for the annular flow has been expressed in terms of the mixture velocity, since $\bar{v}_m$ is the basic variable in the formulation of the general drift-flux model. However, it is also interesting and important to resolve the expression for $\bar{V}_{gj}$ in terms of the total volumetric flux $\langle j \rangle$, since $\langle j \rangle$ was the variable used to correlate $\bar{V}_{gj}$ in dispersed two-phase flow regimes.

By considering the turbulent film-flow regime and using the definition $\langle j_f \rangle = (1 - \langle \alpha \rangle)\langle j \rangle - \langle \alpha \rangle \bar{V}_{gj}$, we can resolve Eq. 85 for the mean drift velocity $\bar{V}_{gj}$. The result does not have a simple form; however, for most practical cases, it can be approximated by a linear function of $\langle j \rangle$:

$$\bar{V}_{gj} \simeq \frac{1 - \langle \alpha \rangle}{\langle \alpha \rangle + \left[\frac{1 + 75(1 - \langle \alpha \rangle)}{\sqrt{\langle \alpha \rangle}} \frac{\rho_g}{\rho_f}\right]^{1/2}} \left[\langle j \rangle + \sqrt{\frac{\Delta \rho g_z D(1 - \langle \alpha \rangle)}{0.015 \rho_f}}\right]. \tag{96}$$

This expression may be further simplified for $\rho_g/\rho_f \ll 1$ as

$$\bar{V}_{gj} \simeq \left(\frac{1 - \langle \alpha \rangle}{\langle \alpha \rangle + 4\sqrt{\rho_g/\rho_f}}\right)\left[\langle j \rangle + \sqrt{\frac{\Delta \rho g_z D(1 - \langle \alpha \rangle)}{0.015 \rho_f}}\right]. \tag{97}$$

From the comparison of Eq. 97 to Eq. 58, the apparent distribution parameter for annular flow becomes

$$C_0 \simeq 1 + \frac{1 - \langle \alpha \rangle}{\langle \alpha \rangle + 4\sqrt{\rho_g/\rho_f}}; \quad (\rho_g/\rho_f \ll 1). \tag{98}$$

This indicates that the apparent C_0 in annular flow should be close to unity.

C. Annular Mist Flow

As the gas velocity increases in the annular flow, the entrainment of liquid from the film to the gas-core flow takes place. Based on recently developed criteria for an onset of entrainment,[51] the critical gas velocity for a rough turbulent film flow can be given by

$$|j_g| > \frac{\sigma}{\mu_f}\sqrt{\frac{\rho_f}{\rho_g}} \times \begin{cases} N_{\mu f}^{0.8} & \text{for } N_{\mu f} \leq \frac{1}{15} \\ 0.1146 & \text{for } N_{\mu f} > \frac{1}{15}, \end{cases} \tag{99}$$

where $N_{\mu f} \equiv \mu_f/[\rho_f \sigma\sqrt{\sigma/g\Delta\rho}]^{1/2}$. However, in general, the vapor flux is much larger than the liquid flux in the annular-mist-flow regime; then, for a weakly viscous fluid such as water or sodium, the above correlation may be replaced by

$$|j_g| \simeq |j| > \left(\frac{\Delta\rho g}{\rho_g^2}\right)^{1/4} N_{\mu f}^{-0.2}. \tag{100}$$

If Inequality 100 is satisfied, then the droplet entrainment into the gas-core flow should be considered; otherwise the correlation for annular flow, Eq. 97, can be applied.

The correlation for $\bar{V}_{gj}$ in annular mist flows can be readily developed by combining the previous results for a dispersed flow and pure annular flow. The area fraction of liquid entrained in the gas core from total liquid area at any cross section is denoted by E_d, and the cross-sectional-area-averaged void fraction by $\langle\alpha\rangle$. Then the film-area fraction is given by

$$1 - \alpha_{core} = \frac{\text{liquid-film cross-sectional area}}{\text{total cross-sectional area}} = (1 - \langle\alpha\rangle)(1 - E_d), \tag{101}$$

and the mean liquid-droplet fraction in the gas core alone is given by

$$\alpha_{drop} = \frac{\text{cross-sectional area of drops}}{\text{cross-sectional area of core}} = \frac{(1 - \langle\alpha\rangle)E_d}{1 - (1 - \langle\alpha\rangle)(1 - E_d)}. \tag{102}$$

Consequently, α_{core} should be used in the annular-flow correlation, Eq. 97, to obtain the relative motion between the core and the film, whereas α_{drop} should be used in the dispersed-flow correlation to obtain a slip between droplets and gas-core flow.

By denoting the gas-core velocity, liquid-drop velocity, and film velocity by v_{gc}, v_{fc}, and v_{ff}, respectively, the total volumetric flux is given by

$$\langle j\rangle = [v_{gc}(1 - \alpha_{drop}) + \alpha_{drop}v_{fc}]\alpha_{core} + v_{ff}(1 - \alpha_{core}). \tag{103}$$

Furthermore, by denoting the total volumetric flux in the core based on the core area by j_{core}, we have from the annular correlation, Eq. 97,

$$j_{core} - \langle j \rangle \simeq \frac{(1 - \langle\alpha\rangle)(1 - E_d)}{\langle\alpha\rangle + 4\sqrt{\rho_g/\rho_f}} \left(\langle j \rangle + \sqrt{\frac{\Delta\rho g_z D(1 - \langle\alpha\rangle)(1 - E_d)}{0.015\rho_f}} \right). \quad (104)$$

On the other hand, from the dispersed-flow correlations, it can be shown that, for a distorted-droplet or churn-droplet flow regime, the drift velocity can be given approximately by

$$\langle\langle v_g \rangle\rangle - j_{core} = \sqrt{2} \left(\frac{\sigma g \Delta\rho}{\rho_g^2} \right)^{1/4} \frac{E_d(1 - \langle\alpha\rangle)}{\langle\alpha\rangle + E_d(1 - \langle\alpha\rangle)}. \quad (105)$$

Here we have used an approximation based on $(1 - \langle\alpha\rangle) \ll 1$. However, depending on the core-gas velocity, the dispersed-flow drift-velocity correlation for a much smaller particle should be used. When the droplets are generated by the entrainment of liquid film, the following approximate form is suggested for an undistorted-particle regime outside the Stokes regime:[44]

$$\langle\langle v_g \rangle\rangle - j_{core} = 0.5 r_d \left[\frac{(g\Delta\rho)^2}{\mu_g \rho_g} \right]^{1/3} \frac{E_d(1 - \langle\alpha\rangle)}{\langle\alpha\rangle + E_d(1 - \langle\alpha\rangle)}, \quad (106)$$

where the particle radius may be approximated from the Weber-number criterion at the shearing-off of wave crests. Thus,

$$r_d \simeq \frac{6\sigma}{\rho_g} \frac{1}{\langle j \rangle^2}. \quad (107)$$

The above relations apply only when the total volumetric flux is sufficiently high to induce fragmentations of the wave crests. Hence, Eq. 106 should be used when

$$|\langle j \rangle| > 1.456 \left(\frac{\sigma g \Delta\rho}{\rho_g^2} \right)^{1/4} \left[\frac{\mu_g^2}{\rho_g \sigma \sqrt{\sigma/g\Delta\rho}} \right]^{-1/12}. \quad (108)$$

By combining the above results, we obtain

$$\bar{V}_{gj} = \frac{(1 - \langle\alpha\rangle)(1 - E_d)}{\langle\alpha\rangle + 4\sqrt{\rho_g/\rho_f}} \left[\langle j \rangle + \sqrt{\frac{\Delta\rho g_z D(1 - \langle\alpha\rangle)(1 - E_d)}{0.015\rho_f}} \right]$$

$$+ \frac{E_d(1 - \langle\alpha\rangle)}{\langle\alpha\rangle + E_d(1 - \langle\alpha\rangle)} \times \begin{cases} \sqrt{2} \left(\frac{\sigma g \Delta\rho}{\rho_g^2} \right)^{1/4} \\ \text{or} \\ \frac{3\sigma}{\rho_g} \left[\frac{(g\Delta\rho)^2}{\mu_g \rho_g} \right]^{1/3} \frac{1}{\langle j \rangle^2}, \end{cases} \quad (109)$$

where the latter expression applies under the condition given by Eq. 108. If the radius of the particle is very small, then the essential contribution to the relative motion between phases comes from the first term of Eq. 109, and the core flow may be considered as a homogeneous dispersed flow. In such a case, Eq. 109 reduces to

$$\bar{V}_{dj} \simeq \frac{(1 - \langle\alpha\rangle)(1 - E_d)}{\langle\alpha\rangle + 4\sqrt{\rho_g/\rho_f}}\left(\langle j\rangle + \sqrt{\frac{\Delta\rho g_z D(1 - \langle\alpha\rangle)(1 - E_d)}{0.015\rho_f}}\right). \tag{110}$$

This expression shows a linear decrease of drift velocity in terms of entrained liquid fraction, which can be observed in various experimental data.[49,50]

VII. COVARIANCE OF CONVECTIVE FLUX

In the one-dimensional drift-flux model, the momentum and energy convective fluxes have been divided into three terms: the mixture convective flux, the drift convective flux, and the covariance term, as can be seen from Eqs. 54 and 55. In other words, the convective flux of quantity ψ for the mixture can be written as

$$\frac{\partial}{\partial z}\left(\sum_k \langle\alpha_k\rho_k\psi_k v_k\rangle\right) = \frac{\partial}{\partial z}(\rho_m\bar{\psi}_m\bar{v}_m) + \frac{\partial}{\partial z}\left(\frac{\langle\alpha_d\rangle\rho_d\rho_c}{\langle\rho_m\rangle}\Delta\psi_{dc}\bar{V}_{dj}\right)$$

$$+ \frac{\partial}{\partial z}\sum_k \mathrm{COV}(\alpha_k\rho_k\psi_k v_k), \tag{111}$$

where $\Delta\psi_{dc} \equiv \langle\langle\psi_d\rangle\rangle - \langle\langle\psi_c\rangle\rangle$ and $\mathrm{COV}(\alpha_k\rho_k\psi_k v_k) \equiv \langle\alpha_k\rho_k\psi_k(v_k - \langle\langle v_k\rangle\rangle)\rangle$. Therefore, for the momentum flux, we have $\psi_k = v_k$ and $\Delta\psi_{dc} = \bar{V}_{dj}/(1 - \langle\alpha_d\rangle)$. On the other hand, for the enthalpy flux, we have $\psi_k = h_k$ and $\Delta\psi_{dc} = \langle\langle h_d\rangle\rangle - \langle\langle h_c\rangle\rangle$, which is equivalent to the latent heat if phases are in thermal equilibrium.

To close the set of the governing equations, we must specify relations for these covariance terms. This can be done by introducing distribution parameters for the momentum and energy fluxes. If we define a distribution parameter for a flux as

$$C_{\psi k} \equiv \frac{\langle\alpha_k\psi_k v_k\rangle}{\langle\alpha_k\rangle\langle\langle\psi_k\rangle\rangle\langle\langle v_k\rangle\rangle}, \tag{112}$$

the covariance term becomes

$$\mathrm{COV}(\rho_k\alpha_k\psi_k v_k) = \rho_k\langle\alpha_k\psi_k(v_k - \langle\langle v_k\rangle\rangle)\rangle = (C_{\psi k} - 1)\rho_k\langle\alpha_k\rangle\langle\langle\psi_k\rangle\rangle\langle\langle v_k\rangle\rangle. \tag{113}$$

For the momentum flux, the distribution parameter is defined by

$$C_{vk} \equiv \frac{\langle \alpha_k v_k^2 \rangle}{\langle \alpha_k \rangle \langle \langle v_k \rangle \rangle^2}. \tag{114}$$

Physically, C_{vk} represents the effect of the void and momentum-flux profiles on the cross-sectional-area-averaged momentum flux of k phase. A quantitative study of C_{vk} can be made by considering a symmetric flow in a circular duct and introducing the power-law expressions in parallel with the analysis of C_0 in Sec. VI.A. Hence we postulate that

$$\frac{\alpha_k - \alpha_{kw}}{\alpha_{k0} - \alpha_{kw}} = 1 - (R/R_w)^n \tag{115}$$

and

$$\frac{v_k}{v_{k0}} = 1 - (R/R_w)^m, \tag{116}$$

where the subscripts 0 and w refer to the value at the centerline and at the wall of a tube.

For simplicity, it is assumed that the void and velocity profiles are similar; i.e., n = m. This assumption is widely used in mass-transfer problems, and it may not be unreasonable for fully developed two-phase flows if one considers that the vapor flux and, hence, the void concentration greatly influence the velocity distributions. Under this assumption, it can be shown that

$$C_{vk} = \frac{\frac{n+2}{n+1}\left(\alpha_{kw} + \Delta\alpha_k \frac{3n}{3n+2}\right)\left(\alpha_{kw} + \Delta\alpha_k \frac{n}{n+2}\right)}{\left(\alpha_{kw} + \Delta\alpha_k \frac{n}{n+1}\right)^2}, \tag{117}$$

where

$$\Delta\alpha_k = \alpha_{k0} - \alpha_{kw}.$$

For a dispersed vapor phase, $\alpha_{gw} \ll \Delta\alpha_g$; hence,

$$C_{vg} \simeq \frac{3n+3}{3n+2}. \tag{118}$$

On the other hand, from Eq. 62, the volumetric-flux-distribution parameter C_0 becomes

$$C_0 \simeq \frac{n+2}{n+1}. \tag{119}$$

Therefore, in the standard range of n, the parameter C_{vg} can be given approximately by

$$C_{vg} \simeq 1 + 0.5(C_0 - 1). \tag{120}$$

For a liquid phase in a vapor-dispersed-flow regime, $\alpha_{fw} \simeq 1$ and $\alpha_{f_0} < 1$. Then from Eq. 117 it can be shown that, for a standard range of α_{f_0} in the bubbly- and churn-flow regimes, C_{vf} can be approximated by

$$C_{vf} = 1 + 1.5(C_0 - 1). \tag{121}$$

For an annular flow, the momentum covariance term can also be calculated by using the standard velocity profiles for the vapor and liquid flows. Thus we obtain

$$C_{vk} \simeq \begin{cases} 1.02 \text{ (turbulent flow)} \\ 1.33 \text{ (laminar flow).} \end{cases} \tag{122}$$

The above result for the individual phases can now be used to study the mixture covariance term. By defining the mixture-momentum-distribution parameter as

$$C_{vm} \equiv \frac{C_{vd}\rho_d\langle\alpha_d\rangle + C_{vc}\rho_c\langle\alpha_c\rangle}{\langle\rho_m\rangle}, \tag{123}$$

the covariance term becomes

$$\sum_k \text{COV}(\alpha_k\rho_k v_k^2) = (C_{vm} - 1)\left[\langle\rho_m\rangle\bar{v}_m^2 + \frac{\rho_c\rho_d\langle\alpha_d\rangle}{(1 - \langle\alpha_d\rangle)\langle\rho_m\rangle}\bar{V}_{dj}^2\right]$$

$$+ \frac{2\rho_c\rho_d\langle\alpha_d\rangle}{\langle\rho_m\rangle}(C_{vd} - C_{vc})\bar{v}_m\bar{V}_{dj}. \tag{124}$$

In view of the above analysis, the order of magnitude of $(C_{vd} - C_{vc})$ is the same as that of $(C_{vm} - 1)$ or less; therefore, the last term on the right-hand side of Eq. 124 can be neglected for almost all cases. This term may be important only in the near critical regime and if $\bar{v}_m \simeq \bar{V}_{dj}$. However,

in general, $\bar{V}_{dj}$ becomes insignificant as the density ratio approaches unity; hence, under the above conditions the convective term itself becomes relatively small. Consequently, even for this case, the term may be dropped. Thus we have

$$\sum_k \mathrm{COV}(\alpha_k \rho_k v_k^2) \simeq (C_{vm} - 1)\left[\langle \rho_m \rangle \bar{v}_m^2 + \frac{\rho_c \rho_d \langle \alpha_d \rangle}{(1 - \langle \alpha_d \rangle)\langle \rho_m \rangle} \bar{V}_{dj}^2\right]. \tag{125}$$

The value of C_{vm} can be evaluated from Eq. 123 by using Eqs. 120 and 121 or Eq. 122. In the bubbly- and churn-flow regimes of practical importance, C_{vm} can be given approximately by

$$C_{vm} \simeq 1 + 1.5(C_0 - 1). \tag{126}$$

However, in the near critical regime C_{vm} depends also on the void fraction and the density ratio. Furthermore, at very low void fractions in a fully developed flow or in a developing flow, the value of C_{vm} should be reduced to the one for the single-phase flow given by Eq. 122. The effect of the development of the void profile into that given by the power law may be taken into account by a similar void-fraction correction term used in the correlation for C_0 in Eq. 70. By recalling that for a turbulent flow $C_{vm} \simeq 1.0$ at $\alpha \to 0$, we obtain for a round tube

$$C_{vm} \simeq 1 + 0.3(1 - \sqrt{\rho_g/\rho_f})\left(1 - e^{-18\langle \alpha \rangle}\right), \tag{127}$$

which may be used both for a fully developed flow and for a developing flow.

On the other hand, for a turbulent-annular-flow regime, we have, from Eqs. 122 and 123, $C_{vm} \simeq 1.02$. For all practical purposes, this may be further approximated by

$$C_{vm} \simeq 1. \tag{128}$$

In reality, the transition from the value given by Eq. 127 to that given by Eq. 128 is a gradual one through the churn-annular (or slug-annular)-flow regime in which characteristics of churn and annular flows alternate. If a single correlation for C_{vm} is preferred, regardless of the flow-regime transitions, then Eq. 127 may be safely extrapolated into higher-void-fraction regime by a simple modification given by

$$C_{vm} = 1 + 0.3(1 - \sqrt{\rho_g/\rho_f})\left[1 - e^{-18\langle \alpha \rangle(1 - \langle \alpha \rangle)}\right]. \tag{129}$$

A similar analysis can be carried out for the enthalpy-covariance term by assuming the void, velocity, and enthalpy profiles. In general,

$$\sum_k \mathrm{COV}(\alpha_k \rho_k h_k v_k) = (C_{hm} - 1)\langle \rho_m \rangle \bar{h}_m \bar{v}_m + \frac{\rho_c \rho_d \langle \alpha_d \rangle}{\langle \rho_m \rangle}\left[-(C_{hc} - 1)\langle\langle h_c \rangle\rangle + (C_{hd} - 1)\langle\langle h_d \rangle\rangle\right]\bar{V}_{dj}, \quad (130)$$

where

$$\begin{cases} C_{hm} \equiv \sum_k C_{hk}\rho_k \langle \alpha_k \rangle \langle\langle h_k \rangle\rangle / (\langle \rho_m \rangle \bar{h}_m) \\ C_{hk} \equiv \langle \alpha_k h_k v_k \rangle / (\langle \alpha_k \rangle \langle\langle h_k \rangle\rangle \langle\langle v_k \rangle\rangle). \end{cases} \quad (131)$$

For a thermal-equilibrium flow, $h_g = h_{gs}$ and $h_f = h_{fs}$, where h_{gs} and h_{fs} are the saturation enthalpies of vapor and liquid. Since in this case the enthalpy profile is completely flat for each phase, the distribution parameters become unity; i.e., $C_{hg} = C_{hf} = C_{hm} = 1$. It is also evident that if one of the phases is in the saturated condition, then C_{hk} for that phase becomes unity.

On the other hand, in the single-phase region, the distribution parameter can be calculated from the assumed profiles for the velocity and enthalpy. Using the standard power-law profiles for a turbulent flow, i.e., $v/v_0 = (y/R)^{1/n}$ and $(h - h_w)/(h_0 - h_w) = (y/R)^{1/m}$, where y is the distance from the wall, we can show that the covariance term is negligibly small both for developing and fully developed flows.

From the above two limiting cases, we can conclude that the enthalpy covariant term may become important only in highly nonequilibrium flow. Even in that case, the energy associated with phase change is considerably larger than that associated with changes in transverse temperature profiles; therefore, except for highly transient cases, the enthalpy covariance can be neglected. Hence,

$$\frac{\partial}{\partial z}\sum_k \mathrm{COV}(\alpha_k \rho_k h_k v_k) \simeq 0. \quad (132)$$

VIII. FLOW-REGIME TRANSITION AND DRIFT VELOCITY IN VERTICAL SYSTEM

In the preceding sections, the drift-velocity correlation has been developed for various two-phase flow regimes. To use this correlation, therefore, we must identify the flow regime first and then choose a suitable expression for $\bar{V}_{dj}$. In the literature for two-phase flow several criteria for

flow-regime transitions are summarized in Refs. 46 and 55-58. These existing criteria may be used to identify the flow regimes under various conditions. However, in what follows, we shall develop flow-regime transition criteria that are based on the relative motion between phases and are consistent with the concept of the drift-flux model.

In forced-convection boiling systems, four flow regimes are of practical importance:[11] churn-turbulent bubbly, annular, annular-mist, and droplet or liquid-dispersed regimes. In the vapor-dispersed-flow regimes such as the bubble, distorted bubbly, and churn-turbulent flows in forced-convection systems, the effect of the concentration and velocity profiles dominates the relative motion between phases. This can be seen from the importance of the term associated with the distribution parameter with respect to the local drift effect in Eq. 58. Consequently, various vapor-dispersed-flow regimes can be satisfactorily represented by the churn-turbulent-flow correlation alone. This is also shown by the experimental data in Figs. 6, 7, 18, 19, and 20.

The transition criterion between churn-turbulent bubbly flow and annular flow is obtained by postulating two different mechanisms for the transition:

1. Flow reversal in the film section along large bubbles and following transport of liquid mass in the slug or wake regions into the film section.

2. Destruction of liquid slugs or large waves by entrainment or deformation and subsequent redistribution of liquid mass into the droplets and film.

The first mechanism assumes that, for the film section along large bubbles, the annular drift-velocity correlation can be used locally. Hence, by setting the flow-reversal condition as $\langle j_f \rangle = 0$ and using Eqs. 46 and 48, we obtain, from Eq. 96,

$$j_g^* = \langle \alpha \rangle^{1.25} \left\{ \frac{1 - \langle \alpha \rangle}{0.015[1 + 75(1 - \langle \alpha \rangle)]} \right\}^{1/2} \simeq \langle \alpha \rangle - 0.1, \tag{133}$$

where $j_g^* = j_g / \sqrt{\Delta \rho g D / \rho_g}$. Here the above approximation is a good fit to the exact form for $\langle \alpha \rangle < 0.93$. At this point, the flow is still in the churn-turbulent regime. It has to support entire liquid fraction in the film in order to have a transition; therefore the mean void fraction is calculated from the drift-velocity correlation for the churn-turbulent flow. Thus from Eq. 76, $\langle \alpha \rangle$ can be obtained in terms of $\langle j_g \rangle$ and $\langle j_f \rangle$. If this expression is substituted into the above equation, we get

$$j_g^* = \frac{1}{C_0 \left\{ 1 + \frac{\langle j_f \rangle}{\langle j_g \rangle} + \frac{\sqrt{2}}{C_0} \frac{1}{\langle j_g \rangle} \left(\frac{\sigma g \Delta \rho}{\rho_f^2} \right)^{1/4} \right\}} - 0.1. \tag{134}$$

In general, the liquid flux and the terminal velocity are much smaller than the gas flux; thus Eq. 134 can be further simplified to

$$j_g^* = \frac{1}{C_0} - 0.1, \tag{135}$$

where C_0 is given by Eq. 68 or 71. Therefore, for a round tube,

$$j_g^* = j_g\sqrt{\frac{\rho_g}{\Delta\rho g D}} = \frac{1}{1.2 - 0.2\sqrt{\rho_g/\rho_f}} - 0.1. \tag{136}$$

The range of j_g^* is accordingly from 0.73 to 0.9. The above value is consistent with various experimental observations.[59-61] For example, Wallis[59] found j_g^* to be 0.8-0.9, and Bennett et al.[61] observed the increase in j_g^* at higher pressures that is predicted by Eq. 136.

The second mechanism of the churn-annular flow-regime transition, which was first suggested by Dukler and Smith,[63] seems to be more applicable to a flow in a larger-diameter tube. In this case, the force balance on the wave crest rather than the liquid motion in the film determines the transition. Since the interfacial geometries are extremely rough at the churn-annular flow-regime transition, the wave deformation or entrainment criterion for a rough turbulent regime developed by Ishii and Grolmes[51] may be used. In this case, the criterion is given by Eq. 99. However, for a nonviscous fluid such as water and sodium, i.e., $N_{\mu f} < 1/15$, Eq. 99 can be rewritten as

$$K \equiv \frac{j_g}{\left(\frac{\sigma g \Delta\rho}{\rho_g^2}\right)^{1/4}} = N_{\mu f}^{-0.2}, \tag{137}$$

where the nondimensional gas flux K is the Kutateladze number[63] and $N_{\mu f} = \mu_f/[\rho_f\sigma\sqrt{\sigma/g\Delta\rho}]^{1/2}$. The value of K does not vary much for most nonviscous fluids, being about 3. The second criterion is valid if the predicted gas flux based on the Kutateladze number is smaller than the one based on the first criterion. This occurs if the following condition is satisfied:

$$D > \sqrt{\frac{\sigma}{\Delta\rho g}} N_{\mu f}^{-0.4} \Big/ \left(\frac{1 - 0.1C_0}{C_0}\right)^2. \tag{138}$$

For water at low pressure, this corresponds approximately to $D > 6$ cm.

The present model gives two different criteria for the churn-annular flow-regime transition: one depending on the diameter of the tube and the other depending only on the properties. This division is qualitatively consistent

with the observation of Pushkina and Sorokin[64] on the breakdown of liquid film, and of Wallis and Kuo[65] on the liquid downward penetration.

The transition between the annular and annular-mist flow can be given by the onset of entrainment.[51] Hence, for nonviscous fluid,

$$|j_g| > \left(\frac{\sigma g \Delta\rho}{\rho_g^2}\right)^{1/4} N_{\mu f}^{-0.2} \times \begin{cases} 11.78 Re_f^{-1/3}; & Re_f \leq 1635, \\ 1; & Re_f > 1635, \end{cases} \tag{139}$$

where $Re_f \equiv \rho_f |\langle j_f \rangle| D/\mu_f$. Figure 23 compares the above criterion to the experimental data.

In an adiabatic system, the transition from an annular flow to a droplet flow is gradual. As the fraction of liquid entrained, E_d, increases, the characteristic of the flow changes from that of a separated flow to a dispersed flow. This trend is clearly exhibited by the expression for the drift velocity in the annular-mist-flow regime, Eq. 109. In other words, the whole annular-mist flow can be considered as a transition regime. On the other hand, in the diabatic system, the occurrence of the critical heat flux and subsequent drying out of the wall introduces a sudden change in flow regimes. If this occurs, Eq. 109 should be used with 100% entrainment or $E_d = 1$.

The recommended drift-velocity correlations for a vertical-boiling flow system are given in Table II.

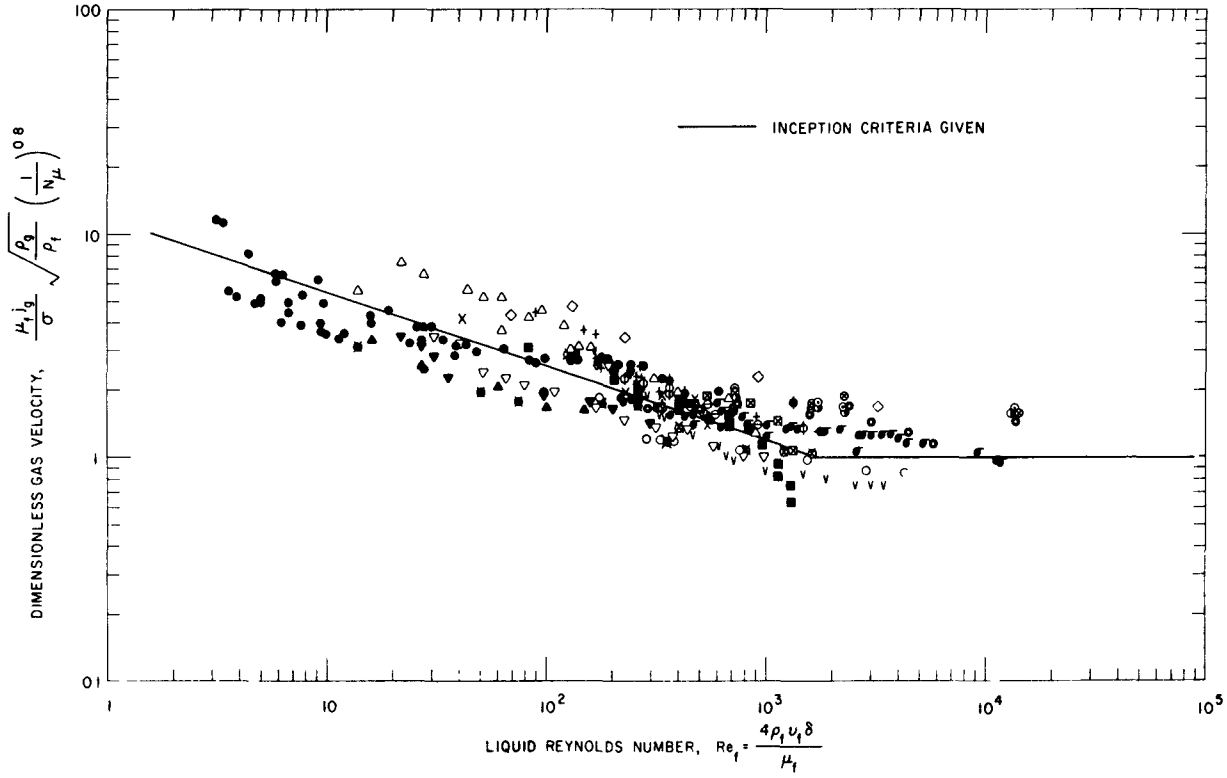

Fig. 23. Comparison of Data for Onset of Entrainment according to Inception Criteria. ANL Neg. No. 900-4572 Rev. 1.

TABLE II Drift Velocity for Vertical Boiling System

Flow Regime	Transition Criteria (Applicable range)	Vapor-drift Velocity, V_{gj}
Churn-turbulent	$\lvert j_g\rvert \le \sqrt{\frac{\Delta\rho g D}{\rho_g}}\left(\frac{1}{C_0} - 0.1\right)$ and $\lvert j_g\rvert \le \left(\frac{\sigma g\Delta\rho}{\rho_g^2}\right)^{1/4} N_{\mu f}^{-0.2}$	$\bar{V}_{gj} = (C_0 - 1)\langle j\rangle + \sqrt{2}\left(\frac{\sigma g\Delta\rho}{\rho_f^2}\right)^{1/4}$, where $C_0 = (1.20 - 0.2\sqrt{\rho_g/\rho_f})(1 - e^{-18\langle\alpha\rangle})$ and $N_{\mu f} = \mu_f/(\rho_f\sigma\sqrt{\sigma/g\Delta\rho})^{1/2}$
Annular	$\sqrt{\frac{\Delta\rho g D}{\rho_g}}\left(\frac{1}{C_0} - 1\right) < \lvert j_g\rvert < \left(\frac{\sigma g\Delta\rho}{\rho_g^2}\right)^{1/4} N_{\mu f}^{-0.2}$	$\bar{V}_{gj} \quad \frac{1 - \langle\alpha\rangle}{\langle\alpha\rangle + 4\sqrt{\rho_g/\rho_f}}\left[\langle j\rangle + \sqrt{\frac{\Delta\rho g D(1 - \langle\alpha\rangle)}{0.015\rho_f}}\right]$
Annular-mist	$\lvert j_g\rvert \ge \left(\frac{\sigma g\Delta\rho}{\rho_g^2}\right)^{1/4} N_{\mu f}^{-0.2}$ and $E_d < 1$	$\bar{V}_{dj} - \frac{(1 - \langle\alpha\rangle)(1 - E_d)}{\langle\alpha\rangle + 4\sqrt{\rho_g/\rho_f}}\left[\langle j\rangle + \sqrt{\frac{\Delta\rho g D(1 - \langle\alpha\rangle)(1 - E_d)}{0.015\rho_f}}\right] + \frac{E_d(1 - \langle\alpha\rangle)}{\langle\alpha\rangle + E_d(1 - \langle\alpha\rangle)} \times \begin{cases} \sqrt{2}\left(\frac{\sigma g\Delta\rho}{\rho_g^2}\right)^{1/4} \\ \text{or} \\ \frac{3\sigma}{\rho_g}\left[\frac{(g\Delta\rho)^2}{\mu_g\rho_g}\right]^{1/3}\frac{1}{\langle j\rangle^2} \end{cases}$ The second expression applies when $\lvert j\rvert > 1.456\left(\frac{\sigma g\Delta\rho}{\rho_g^2}\right)^{1/4}\left(\frac{\mu_g^2}{\rho_g\sigma\sqrt{\sigma/g\Delta\rho}}\right)^{-1/12}$
Liquid dispersed	$E_d = 1.0$ or $q''_w > q''_{cr}$	$\bar{V}_{gj} - (1 - \langle\alpha\rangle) \times \begin{cases} \sqrt{2}\left(\frac{\sigma g\Delta\rho}{\rho_g^2}\right)^{1/4} \\ \text{or} \\ \frac{3\sigma}{\rho_g}\left[\frac{(g\Delta\rho)^2}{\mu_g\rho_g}\right]^{1/3}\frac{1}{\langle j\rangle^2} \end{cases}$

IX. CONCLUSIONS

For a dispersed two-phase flow system, the relative motion between phases has been analyzed by considering the drag force, the gravitational force, and the effect of the pressure gradient due to shear stresses, and using a similarity hypothesis based on the Reynolds number and drag coefficient. The effect of the multiparticle system is taken into account by using the mixture viscosity in the Reynolds number. The present model for the relative motion between phases has been developed for general dispersed two-phase flows; therefore its applicability is not limited to particulate flows, but it can also be applied to bubbly and droplet flows. For solid-particle systems, it agrees with experimental data at all Reynolds-number and particle-concentration ranges of practical interest. Furthermore, the present theory can be reduced to the existing theoretical model for a solid-particle system in the Stokes regime by considering the limiting case of small particles.

On the other hand, for fluid-particle systems, considering bubbly flows in a vertical channel, the present model can be essentially reduced to conventional semiempirical correlations. Consequently, the relative motion between phases in dispersed two-phase flows can be predicted by the unified theory for both solid- and fluid-particle systems at all ranges of Reynolds numbers.

For annular flow, the constitutive equation for the drift velocity was developed by taking into account the effect of gravity, interfacial shear stress with its dependence on interfacial roughness, and flow regimes in the liquid film. The constitutive equation obtained in this report is cast into two different forms: one useful for analyzing steady-state flows and the other for transient flows. The predicted vapor-drift velocity from this study was compared to about 350 data points from various experiments. Although the data used in the comparison included those taken in the drop-annular-flow regimes with moderate entrainment, the theoretical predictions were within ±30% of the measured values. However, when the amount of liquid entrainment was large, the present correlation overpredicted the vapor-drift velocity. However, this trend can easily be explained by a newly developed correlation for an annular dispersed-flow regime that shows an almost linear decrease of drift velocity in terms of entrained liquid mass.

The present constitutive equations for the drift velocity in various two-phase-flow regimes have been obtained from the steady-state and adiabatic formulations. The effects of heat transfer and phase changes on the drift velocity were considered secondary. These effects appear only indirectly through the local variables, such as the void fraction and the mixture velocity in the drift constitutive equation. It is a common practice to apply constitutive relationships obtained under steady-state conditions to the transient problems, with an assumption that the parameters entering into a constitutive relationship are local variables and are functions of time. Therefore, the application of the present constitutive equation for the drift velocity to the transient two-phase flow with a phase change will be consistent with the common practice.

However, the basic assumption of the drift-flux model is that a strong coupling exists between the motions of two phases. Therefore, certain two-phase problems involving a sudden acceleration of one phase may not be appropriately described by this model. In these cases, inertia terms of each phase should be considered separately, that is, by use of a two-fluid model. However, the real usefulness of the drift-flux model in many practical engineering problems comes from the fact that even two-phase mixtures that are weakly coupled locally are strongly coupled when considered as a total system. This is because the relatively large axial extent of the systems usually gives sufficient interaction times for the momentum exchange between two phases.

APPENDIX

Relative Motion in Single-particle System

A motion of the single solid particles, drops, or bubbles in an infinite medium has been studied extensively in the past. (See, for example, Refs. 52-54.) In what follows, we shall summarize these results in simple forms useful for the development of the drift constitutive equation in multiparticle systems.

By denoting the relative velocity of a single particle in an infinite medium by $v_{r\infty} = v_d - v_{c\infty}$, we define the drag coefficient by $C_{D\infty} \equiv -2F_D/\rho_c v_{r\infty}|v_{r\infty}|\pi r_d^2$, where F_D is the drag force and r is the radius of a particle. On the other hand, the sum of the pressure and body forces acting on the particle is given by

$$F_p + F_g = \tfrac{4}{3}\pi r_d^3(\rho_c - \rho_d)g \tag{A.1}$$

which should be balanced by the drag force. Hence, $F_p + F_g + F_D = 0$. By introducing the nondimensional parameters for the velocity fields and radius given by $v^* \equiv |v|(\rho_c^2/\mu_c g\Delta\rho)^{1/3}$ and $r_d^* \equiv r_d(\rho_c g\Delta\rho/\mu_c^2)^{1/3}$, we can solve the force balance for the radius as

$$r_d^* = \tfrac{3}{8}C_{D\infty}v_{r\infty}^{*2}. \tag{A.2}$$

The standard particle Reynolds number and the viscosity number are defined by

$$\left.\begin{aligned} N_{Re\infty} &\equiv \frac{2r_d\rho_c|v_{r\infty}|}{\mu_c} = 2r_d^*v_{r\infty}^* \\ \text{and} \qquad & \\ N_\mu &\equiv \mu_c \Big/ \left(\rho_c\sigma\sqrt{\frac{\sigma}{g\Delta\rho}}\right)^{1/2} \end{aligned}\right\}, \tag{A.3}$$

where N_μ measures the viscous force induced by a flow to the surface-tension force.[66] Extensive studies of the single-particle drag show that, in general, the drag coefficient is a function of the Reynolds number. However, the exact functional form depends on whether the particle is a solid particle, drop, or bubble.

For a viscous regime, the function $C_{D\infty}$ is given by

$$C_{D\infty} = \frac{24}{N_{Re\infty}}\left(1 + 0.1N_{Re\infty}^{0.75}\right). \tag{A.4}$$

For solid particles, the drag coefficient becomes essentially constant at approximately $C_{D\infty} = 0.45$ for $N_{Re\infty} \geq 1000$. This Newton's regime holds up to $N_{Re\infty} = 2 \times 10^5$.

For fluid particles such as drops or bubbles, the flow regime is characterized by the distortion of particle shapes and irregular motions. In this distorted-particle regime, the experimental data show that the terminal velocity is independent of particle size. From this it can be seen that the drag coefficient $C_{D\infty}$ does not depend on the viscosity, but should be proportional to the radius of the particle. Physically this indicates that the drag force is governed by the distortion and swerving motion of the particle, and the change of the particle shape is toward an increase in the effective cross section. Therefore, $C_{D\infty}$ should be scaled by the mean radius of the particle rather than the Reynolds number.[52] Then,

$$C_{D\infty} = \tfrac{4}{3} r_d \sqrt{g\Delta\rho/\sigma} \quad \left(\text{or } C_{D\infty} = \tfrac{4}{3} N_\mu^{2/3} r_d^*\right) \tag{A.5}$$

for $N_\mu \geq 36\sqrt{2}(1 + 0.1N_{Re\infty}^{0.75})/N_{Re\infty}^2$. However, since the terminal velocity in this regime can be uniquely related to physical properties, Eq. A.5 can be rewritten in terms of the terminal velocity or the Reynolds number as

$$C_{D\infty} = \frac{2\sqrt{2}}{3} N_\mu r_d^* v_{r\infty}^* \quad \left(\text{or } C_{D\infty} = \frac{\sqrt{2}}{3} N_\mu N_{Re\infty}\right). \tag{A.6}$$

Note that the above expression is a special form based on the solution of the balance between drag and gravity forces and it may not be used in more general situations. As the size of bubbles further increases, the bubbles become spherical-cap shaped and the drag coefficient reaches a constant value of $C_{D\infty} = 8/3$. The transition from the distorted-bubble regime to the spherical-cap bubble regime occurs at around $r_d^* = 2/N_\mu^{2/3}$. For a liquid drop, the drag coefficient can increase further according to Eq. A.5; however, eventually a droplet becomes unstable and disintegrates into smaller drops. This limit can be given by the well-known Weber-number criterion, and it corresponds to $r_d^* \leq 3/N_\mu^{2/3}$ and $C_{D\infty} \leq 4$. The above results on the drag coefficient for single particles of solid, liquid, and gas are summarized in Fig. 1.

By knowing the drag law, $C_{D\infty} = C_{D\infty}(N_{Re\infty})$, we can calculate the terminal velocity from Eq. A.2). In the viscous regime, the terminal velocity can be approximated by

$$v_{r\infty}^* \simeq \frac{4.86}{r_d^*}\left[(1 + 0.08 r_d^{*3})^{4/7} - 1\right]. \tag{A.7}$$

On the other hand, in Newton's regime for solid particles, the drag coefficient is constant; therefore,

$$v^*_{r\infty} = 2.43 r^{*1/2}_d, \tag{A.8}$$

which holds for $r^*_d \geq 34.65$.

For the distorted-fluid-particle regime, the terminal velocity reduces to a constant value of

$$v^*_{r\infty} = \sqrt{2}/N^{1/3}_\mu. \tag{A.9}$$

Hence, in this regime, the relative velocity is independent of the fluid-particle size. Furthermore, for the spherical-cap bubble regime, the terminal velocity becomes

$$v^*_{r\infty} = r^{*1/2}_d \tag{A.10}$$

These results are summarized in Fig. 2.

ACKNOWLEDGMENTS

I would like to express my appreciation to Dr. N. Zuber of NRC for valuable discussions on the subject. I am also indebted to Drs. M. A. Grolmes, D. Condiff, and T. C. Chawla for having discussed various aspects of the analysis.

REFERENCES

1. J. M. Delhaye, *Equations fondamentales des écoulements diphasiques*, Part 1 and 2, CEA-R-3429, France (1968).
2. P. Vernier and J. M. Delhaye, *General Two-Phase Flow Equations Applied to the Thermohydrodynamics of Boiling Nuclear Reactor*, Energ. Prim. *4*(1) (1968).
3. J. Bouré and M. Réocruex, "General Equations of Two-phase Flows," *4th All Union Heat and Mass Transfer Conference*, Minsk, USSR (1972).
4. M. Ishii, *Thermo-fluid Dynamic Theory of Two-phase Flow*, Chapters IX and X, Eyrolles, Paris, Scientific and Medical Publication of France, N. Y. (1975).
5. M. Réocreux, *Contribution à l'étude des débits critiques en éculement diphasique eau vapeur*, Ph.D. thesis, University of Grenoble, France (1974).
6. N. Zuber, "Flow Excursions and Oscillations in Boiling, Two-phase Flow Systems with Heat Addition," *Proc. Symp. Two-phase Flow Dynamics*, Vol. 1, p. 1071 (1967).
7. N. Zuber and D. E. Dougherty, "Liquid Metals Challenge to the Traditional Methods of Two-phase Flow Investigations," *Proc. Symp. Two-phase Flow Dynamics*, Vol. 1, p. 1090 (1967).
8. M. Ishii, O. Jones, and N. Zuber, *Thermal non-equilibrium Effects in Drift Flux Model of Two-phase Flow*, Trans. Am. Nucl. Soc. *22*, 263 (1975).
9. N. Zuber, *On the Dispersed Two-phase Flow on the Laminar Flow Regime*, Chem. Eng. Sci. *19*, 897 (1964).
10. N. Zuber and J. A. Findlay, *Average Volumetric Concentration in Two-phase Flow Systems*, J. Heat Transfer *87*, 453 (1965).
11. N. Zuber, F. W. Staub, G. Bijwaard, and P. G. Kroeger, *Steady State and Transient Void Fraction in Two-phase Flow Systems*, General Electric Co. Report GEAP-5417, Vol. 1 (1967).
12. M. Ishii, T. C. Chawla, and N. Zuber, *Constitutive Equation for Vapor Drift Velocity in Two-phase Annular Flow*, AIChE J. *22*, 283 (1976).
13. G. F. Carrier, *Shock Waves in a Dusty Gas*, J. Fluid Mech. *4*, 376 (1958).
14. W. D. Rannie, "Perturbation Analysis of One-Dimensional Interogeneous Flow in Rocket Nozzles," *Detonation and Two-Phase Flow*, Academic Press, New York (1962).
15. J. M. Burgers, Proc. K. Med. Akad. Wet. *44*, 1045 (1941); *45*, 9 (1942).
16. P. G. W. Hawksley, "The Effect of Concentration on the Settling of Suspensions and Flow through Porous Media," *Some Aspects of Fluid Flow*, p. 114, Edward Arnold, London (1951).

17. H. Brinkman, *Viscosity of Concentrated Suspensions and Solutions*, J. Chem. Phys. *20*, 571 (1952).

18. R. Roscoe, *The Viscosity of Suspensions of Rigid Spheres*, Br. J. Appl. Phys. *3*, 267 (1952).

19. R. F. Landel, B. G. Moser, and A. J. Bauman, "Rheology of Concentrated Suspensions: Effects of a Surfactant," *4th Int. Congress on Rheology, Brown Univ., Proc.*, Part 2, p. 663 (1965).

20. N. A. Frankel and A. Acrivos, *On the Viscosity of a Concentrated Suspension of Solid Spheres*, Chem. Eng. Sci. *22*, 847 (1967).

21. H. Eilers, Kolloid-Z *97*, 313 (1941).

22. D. G. Thomas, *Transport Characteristics of Suspension: VIII*, J. Colloid Sci. *20*, 267 (1965).

23. J. F. Richardson and W. N. Zaki, *Sedimentation and Fluidization: Part 1*, Trans. Inst. Chem. Eng. *32*, 35 (1954).

24. M. Ishii, *Thermally-induced Flow Instabilities in Two-phase Mixtures in Thermal Equilibrium*, Ph.D. thesis, Georgia Institute of Technology (1971).

25. D. J. Nicklin, J. O. Wilkes, and J. F. Davidson, *Two-phase Flow in Vertical Tubes*, Trans. Inst. Chem. Eng. *40*, 61 (1962).

26. L. G. Neal, *An Analysis of Slip in Gas-liquid Flow Applicable to the Bubble and Slug Flow Regimes*, Report KR-2 Kjeller Research Establishment, Norway (1963).

27. S. G. Bankoff, *A Variable Density Single-fluid Model for Two-phase Flow with Particular Reference to Steam-water Flow*, J. Heat Transfer, Trans. ASME *82*, 265 (1960).

28. T. A. Hughes, *Steam-Water Mixture Density Studies in a Natural Circulation High Pressure System*, Babcock and Wilcox, G. Report No. 5435 (1958).

29. R. J. Thome, *Effect of a Transverse Magnetic Field and Vertical Two-phase Flow through a Rectangular Channel*, ANL-6854 (Mar 1964).

30. G. E. Smissaert, *Two-component Two-phase Flow Parameters for Low Circulation Rates*, ANL-6755 (July 1963).

31. M. Petrick, *A Study of Vapor Carryunder and Associated Problems*, ANL-6581 (July 1962).

32. F. Bergonzoli, and F. J. Halfen, *Heat Transfer and Void Formation during Forced Circulation Boiling of Organic Coolants*, NAA-SR-8906, Atomics International (1964).

33. W. T. Hancox, and W. B. Nicoll, *Prediction of Time-dependent Diabatic Two-phase Water Flows*, Prog. Heat Mass Transfer *6*, 119 (1972).

34. J. Nikuradse, *Gesetzmäsigkeit der turbulenten strömung in glatten Rohren*, Forsch. Arb. Ing.-Wes. *356* (1932).

35. G. W. Maurer, *A Method of Predicting Steady State Boiling Vapour Fractions in Reactor Coolant Channels*, WAPD-BT-19 (1956).

36. G. B. Wallis, D. A. Steen, S. N. Brenner, and T. M. Turner, *Joint U. S.-Euratom Research and Development Program, Quarterly Progress Report, January, Dartmouth College* (1964).

37. S. C. Rose, and P. Griffith, *Flow Properties of Bubbly Mixtures*, ASME Paper 65-HT-8 (1965).

38. N. Adorni, G. Peterlongo, R. Ravetta, and F. A. Tacconi, *Large Scale Experiments on Heat Transfer and Hydrodynamics with Steam-Water Mixtures*, CISE Report R-91, Italy (1964).

39. S. Z. Rouhani, and K. M. Becker, *Measurement of Void Fractions for Flow of Boiling Heavy Water in a Vertical Round Duct*, AE-106, Aktiebolaget Atomenergi, Sweden (1963).

40. K. Schwartz, *Investigation of Distribution of Density, Water and Steam Velocity and of the Pressure Drop in Vertical Horizontal Tubes*, VDI Forschungsh. *20*, Series B, 445 (1954).

41. C. C. St. Pierre, *Frequency-response Analysis of Steam Voids to Sinusoidal Power Modulation in a Thin-walled Boiling Water Coolant Channel*, ANL-7041 (May 1965).

42. J. F. Marchaterre, *The Effect of Pressure on Boiling Density in Multiple Rectangular Channels*, ANL-5522 (Feb 1956).

43. J. L. L. Baker, *Flow-regime Transitions at Elevated Pressures in Vertical Two-phase Flow*, ANL-7093 (Sept 1965).

44. M. Ishii, "One-dimensional Drift-flux Modeling: One-dimensional Drift Velocity of Dispersed Flow in Confined Channel," *Light-water-reactor Safety Research Program: Quarterly Progress Report, January-March 1976*, ANL-76-49, p. 1, (1976).

45. D. T. Dumitrescu, *Stomung an einer Luftblase in senkrechten Rohr*, Z. Angew. Math. Mech. *23*, 139 (1943).

46. G. B. Wallis, *One-dimensional Two-Phase Flow*, McGraw-Hill Book Co., Inc., New York (1969).

47. H. Fauske, "Critical Two-phase, Steam Water Flow," *Proc. Heat Transfer and Fluid Mechanics Institute*, Stanford Univ. Press, Calif., p. 78 (1962).

48. L. E. Gill, and G. F. Hewitt, *Further Data on the Upwards Annular Flow of Air-water Mixtures*, UKAEA Report AERE-R3935 (1962).

49. P. Alia, L. Cravarolo, A. Hassid, and E. Pedrocchi, *Liquid Volume Fraction in Adiabatic Two-phase Vertical Upflow-Round Conduit*, CISE Report-105, Italy (1965).

50. L. Cravarolo, A. Giorgini, A. Hassid, and E. Pedrocchi, *A Device for the Measurement of Shear Stress on the Wall of a Conduit; Its Application in the Mean Density Determination in Two-phase Flow; Shear Stress Data in Two-phase Adiabatic Vertical Flow*, CISE Report-82, Italy (1964).

51. M. Ishii, and M. A. Grolmes, *Inception Criteria for Droplet Entrainment in Two-Phase Concurrent Film Flow*, AIChE J. *21*, 308 (1975).

52. F. N. Peebles, and H. J. Garber, *Studies on the Motion of Gas Bubbles in Liquid*, Chem. Eng. Prog. *49*, 88 (1953).

53. T. Z. Harmathy, *Velocity of Large Drops and Bubbles in Media of Infinite and Restricted Extent*, AIChE J. *6*, 281 (1960).

54. G. B. Wallis, *The Terminal Speed of Single Drops or Bubbles in an Infinite Medium*, Int. J. Multiphase Flow *1*, 491 (1974).

55. G. F. Hewitt, and N. S. Hall-Taylor, *Annular Two-Phase Flow*, Pergamon Press, New York (1970), pp. 1-20.

56. J. G. Collier, *Convective Boiling and Condensation*, pp. 14-18, McGraw-Hill Book Co., Inc., New York (1972).

57. G. W. Govier, and K. Aziz, *Flow of Complex Mixtures in Pipe*, Van Nostrand Reinhold Co., New York, pp. 335-337, (1972).

58. Y. Taitel, and A. E. Dukler, *Flow Regime Transitions for Vertical Upward Gas Liquid Flow*, NUREG-0162 and -0163, University of Houston (1977).

59. G. B. Wallis, *Transition from Flooding to Upwards Cocurrent Annular Flow in a Vertical Pipe*, UKAEA Report AEEW-R 142 (1962).

60. G. F. Hewitt, H. A. Lacey, and B. Nichols, "Transition in Film Flow in a Vertical Tube," *Symp. Two-phase Flow*, Exter, Vol. 2, Paper B4 (1965).

61. A. W. Bennett, G. F. Hewitt, H. A. Kearsey, R. F. Keeys, and P. C. Lacey, *Flow Visualization Studies of Boiling at High Pressure*, UKAEA Report AERE-R4874 (1965).

62. A. E. Dukler and L. Smith, *Two-phase Interactions in Countercurrent Flow Studies of the Flooding Mechanism*, University of Houston Report AT 49-24 0194 (1976).

63. S. S. Kutateladze, *Elements of the Hydrodynamics of Gas-Liquid Systems*, J. Fluid Mech. Soviet Res. *1*(4), 29 (1972).

64. O. L. Pushikina and Y. L. Sorokin, *Breakdown of Liquid Film Motion in Vertical Tubes*, J. Heat Transfer Soviet Res. *1*, 56 (1969).

65. G. B. Wallis and J. T. Kuo, *The Behavior of Gas-liquid Interfaces in Vertical Tubes*, Int. J. Multiphase Flow *2*, 521 (1976).

66. C. A. Sleicher, Jr., *Maximum Stable Droplet Size in Turbulent Flow*, AIChE J. *8*, 471 (1972).